Nano Energy (▮▮▮▮) ▮, ▮▮▮–▮▮▮

Available online at www.sciencedirect.com

SciVerse ScienceDirect

journal homepage: www.elsevier.com/locate/nanoenergy

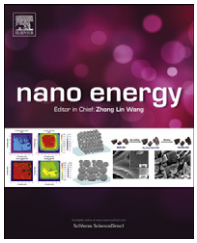

REVIEW

A review on the enhancement of figure of merit from bulk to nano-thermoelectric materials

Hilaal Alam[a,*], Seeram Ramakrishna[b]

[a]Qtech Nanosystems Pte. Ltd, Singapore
[b]FREng, FNAE, National University of Singapore, Singapore

Received 22 August 2012; received in revised form 12 October 2012; accepted 13 October 2012

KEYWORDS
Seebeck;
Thermoelectric;
Nanocomposites;
Microelectronics;
Power generation;
Thermal management

Abstract
Thermal management and energy crisis have been two major problems in this 21st century. The thermoelectric concept is seen as a perfect solution for the both issues provided its figure of merit is large enough to compete with the traditional techniques. Since the use of semiconductor materials for thermoelectric applications, there has been a huge quest for improving its figure of merits (ZT) to cross 3 in order to make it commercially viable. This review starts with thermoelectric concepts and explains briefly the challenges in enhancing the figure of merits. It also reports the various approaches adopted in bulk materials, complex structures and the recent nanostructures to circumvent the interdependency of parameters in achieving higher ZT. It ends with discussion of the future trends of nanocomposite materials and its underlying challenges of fabrication.

Introduction

Researchers and industries are throwing their efforts and resources to find solutions for the escalating energy crisis and the threatening global warming. One of the ways to tackle these issues lies in achieving higher efficient thermal management which solves several other issues in tandem. A solid state or semiconductor electronics component, for example, can perform reliably well for many years when they are operating at or near the ambient temperature. Due to the advancement of semiconductor lithography and dense packaging, the heat generation in chips is nearly touching 100 W/cm^2 [1]. Bar-Cohen et al. showed that for every 2° K rise of temperature, the reliability of the silicon chip decreases by 10% [2]. A U.S. Air Force study indicated that more than 50% of the electronic failures are temperature-related [3]. The thermal problem has, thus become one of the major limiting factors of scaling of CMOS and hence it is essential for thermal management and logic-flow to be considered concurrently for system level approaches [4].

The thermoelectric is a promising technique to convert the waste thermal energies into useful power as well as to cool ambience without using harmful chemicals like CFC and

Abbreviations: CMOS, complementary metal oxide semiconductor; ZT, figure of merits; TE, thermoelectric

*Correspondence to: 200, Jalan Sultan # 13-10, 199018 Singapore, Singapore. Tel.: +65 83751070; fax: +65 6281 7761.
E-mail addresses: hilaal@qtechnanosystems.com, alam.hilaal@gmail.com (H. Alam).

2211-2855/$ - see front matter © 2012 Elsevier Ltd. All rights reserved.
http://dx.doi.org/10.1016/j.nanoen.2012.10.005

Please cite this article as: H. Alam, S. Ramakrishna, A review on the enhancement of figure of merit from bulk to nano-thermoelectric materials, Nano Energy (2013), http://dx.doi.org/10.1016/j.nanoen.2012.10.005

Nomenclature

S	Seebeck coefficient	k_b	Boltzmann constant
E	charge—coulomb	h	Plank constant
T	temperature—Kelvin	m	effective mass of charge carriers
I	current—amp	k_o	electronic thermal conductivity electrochemical potential gradient is zero
Q	Heat	E	energy
Z	figure of merit -/K	σ	electric conductivity
ZT	figure of merit (dimensionless)	τ'	relaxation time
K	thermal conductivity	P	electric resistivity
K_e	electronic thermal conductivity	μ	carrier mobility
K_{th}	Lattice Thermal conductivity	$\prod$	Peltier coefficient
L	Lorenz factor 2.4×10^{-8} J^2/K^2C^2	τ	Thomson coefficient
N	number of charge carriers	Λ	scattering parameter
		τ_0	energy-independent scaling co-efficient

moving parts. It is, however, already in use to cool diode lasers [5], critical electronics [6], portable refrigeration [7], cool/ heat car seats and even railway passenger cars in France [8] where the cost is not a primary concern. Thermoelectric cooling is also used to produce $-80\,^{\circ}C$ temperature to operate the sensors in infrared imaging systems for heat-seeking missiles and night-vision systems [9]. In life science biological assaying has been revolutionized with the development of polymerase chain reaction (PCR) systems which use thermoelectric to thermally cycle microliter quantities of enzymatic reactions through the exact series of temperature cycles. The process is used to multiply specific sequence of DNA materials for analytical purposes [10].

In the other direction, thermoelectric generators are chosen for generating power because of its reliable, maintenance free operations. It is also used when the durability with longer operating life under extreme conditions are required. The silicon germanium—the high temperature power generation materials—led directly to the production of heat engines with no moving part for space application that could operate even in the absence of the sun. Although the solar cells are used in spacecraft, they are useful only for the short distance up to the Mars and beyond where the solar radiant flux is not adequate, thermoelectric takes over to generate the power. All the power sources for US and former USSR deep-space probes have used thermoelectric heat engines to convert heat generated by nuclear fissile materials to electricity [11,12] Micro-thermoelectric generator are used in many low power devices such as hearing aids and wrist watches. Recently Seiko and Citizen introduced commercialized thermoelectrically driven low power wrist watches [12].

A report informs that 69% of energy demand is for heating/ cooling and electricity. 191 million vehicles strong US, dissipate 66% of their energy as heat through emission and about 36 TWh of waste process heat per year in USA [13]. Thus a huge amount of waste heat from automotive, industry operations, and mankind activities can be converted into the useful energy with TE. However, the figure of merit ZT of the thermoelectric materials should reach well above 3 from the current~1.5 to 2, in order to compete with the traditional techniques [14] such as vapor compression machines.

Law of thermoelectric effects

The phenomenon involving a direct energy conversion from heat into electricity (or vice versa) is known as thermoelectric effect. In 1821 Thomas Seebeck discovered the generation of voltage when a conductor was subjected to a temperature gradient and converted the thermal energy into electricity with the efficiency of about 3% [15]. An electromotive force is generated due to the charge carrier diffusion and phonon drag between two extreme temperatures (Fig. 1). Actually, the whole systems is in semi-equilibrium i.e. chemical potential (μ) due to the concentration is balanced by the built-in electrostatic potential which is known as Seebeck voltage [16]. The change in electrochemical potential ($\partial_x\mu$) in x direction per unit charge 'e' per unit temperature (∂T) defines the Seebeck coefficient (S) [17],

$$S = \frac{1}{e}\frac{\partial_x \mu}{\partial T} \tag{i}$$

The reversal of this phenomenon is known as Peltier effect ($\prod$) which is a measure of the amount of heat (Q) carried by electrons or holes and is proportional to the electrical current (I) flowing in the circuit [18].

$$\Pi = \frac{Q}{I} \tag{ii}$$

The Seebeck effect and the Peltier effects can be described with what is known as the Thomson effect that explains the heating or cooling of a current carrying material subject to a temperature gradient. More specifically heat is liberated if an electric current flows in the same direction as the heat flows; otherwise it is absorbed. The Thomson coefficient 'τ' can be defined as [18]

$$\frac{dQ}{dx} = \tau I \frac{dT}{dx} \tag{iii}$$

Figure 1 Charge transportation from the hot to cold end for negative Seebeck co-efficient materials.

Please cite this article as: H. Alam, S. Ramakrishna, A review on the enhancement of figure of merit from bulk to nano-thermoelectric materials, Nano Energy (2013), http://dx.doi.org/10.1016/j.nanoen.2012.10.005

where dQ/dx is the rate of heating (or cooling) per unit length, I is the electric current and dT/dx is the temperature gradient. The Seebeck coefficient becomes negative when electrons diffuse from hot end to populate the cold end with electrons. The performance of the thermoelectric materials is often denoted as figure of merit Z whose unit is K^{-1}, or ZT the dimensionless unit [19].

$$ZT = \frac{\sigma S^2}{K_e + K_{th}} T \quad \text{(iv)}$$

where σ is electric conductivity and $K=K_e+K_{th+}K_{bi}$. K_e is thermal conductivity due to electron transport, K_{th} is the thermal conductivity due to the lattice phonon. The thermal conductivity is also contributed by the bipolar effect K_{bi}. From the Eq. (iv), the absence of the thermal conductivity causes ZT to reach infinity and the thermoelectric devices to approach the Carnot cycle efficiency. In ZT, the energy carriers such as electrons and holes, contribute to electric conductivity (σ) and electronic thermal conductivity (k_e) while the phonons contribute to the lattice thermal conductivity(K_{th}). It is also found that commercially available materials those have ZT$\sim$1 cannot compete with the traditional vapor compression systems when operating at a relatively larger temperature lift or difference (T_H-T_C), e.g. 30 °C. However, decreasing the temperature lift, the efficiency of thermoelectric modules increases rapidly. It is expected that the efficiency of thermoelectric modules could eventually surpass that of traditional vapor compression and possibly all other competing concepts when temperature lift is very small such as 5 °C [20]. Moreover, it is encouraging to know that the second law of thermodynamics does not impose any restriction on increasing the value of ZT and yet, it has been difficult to cross ZT beyond certain point [21].

Challenges in enhancing ZT

The best thermoelectric materials were succinctly defined as "phonon-glass electron-crystal" (or PGEC in short), which means that the materials should have a low lattice thermal conductivity as in a glass, and a high electrical conductivity as in a crystal [22]. The interdependency of the TE parameters makes the enhancement efforts of ZT very challenging. The normal ways of optimizing TE materials are to increase the power factor $S^2\sigma$ by optimizing the carrier concentration n, and/ or to reduce the lattice thermal conductivity K_{th} by introducing the scattering centers. These parameters are the function of scattering factor r, carrier effective mass m^* and carrier mobility μ and their interconnectivity limit ZT to about 1 in large bulk materials.

According to the kinetic definition S is the energy difference between the average energy of mobile carrier and the Fermi energy [23]. If the carrier concentration n is increased, the Fermi energy as well as the average energy increases. However, the Fermi energy increases more rapidly than the average energy when n is increased. As a result S decreases, dragging the power factor (S^2n) down rapidly. Thus in attempting to increase ZT for most of the homogeneous materials, the carrier concentration (n) increases electrical conductivity (σ) but reduces the Seebeck coefficient (S). For this reason, in metals and degenerate semiconductors (energy-independent scattering approximation), the Seebeck coefficient can be expressed as [24]

$$S = \frac{8\pi^2 k_B^2}{3eh^2} m^* T \left(\frac{\pi}{3n}\right)^{\frac{2}{3}} \quad \text{(v)}$$

The parameter m* is density of states effective mass in the Eq. (v). The high m* influence the power factor to raise according to the Eq. (v). Most materials having high m* have generally low μ which limits the power factor by a weighted mobility with the relationship of power factor proportional to $(m^*)^{3/2}\mu$. Also, there is no such thing as an optimal effective mass. There are low mobility high effective mass polaron conductors (oxides, chalcogenides) as well as high mobility low effective mass semiconductors (SiGe, GaAs) [25].

It should also be noted that the defects scatter not only the phonons but also the electrons. Hence there are some trade-offs carried out in carrier mobility when designing for reducing lattice thermal conductivity. The ratio of μ/K_{th} determines the improvement of ZT [15]. Although the increase in the ratio is usually experimentally achieved through a more reduction in K_{th} rather than that in μ, some fundamental issues in this mechanism are not understood well[?].

Wiedemann-Frenz Law states that [25] the electronic contribution to the thermal conductivity is proportional to the electrical conductivity of the materials and the relationship is

$$K_e/\sigma = LT \quad \text{(vi)}$$

where L is Lorenz factor 2.4×10^{-8} J^2/K^2C^2 for free electrons and this can vary particularly with carrier concentration. The electrical resistivity (ρ) is related to the carrier concentration 'n', electron charge 'e' and chemical potential 'μ' as [25]

$$\frac{I}{\rho} = \sigma = \mu ne \quad \text{(vii)}$$

The electronic thermal conductivity can thus be expressed as

$$K_e = \sigma LT = \mu neLT \quad \text{(viii)}$$

This relationship shows that the low carrier concentration will result into the lower electrical conductivity decreasing ZT. High mobility carriers are most important for high value of electrical conductivity. Again from the Eqs. (v), it is shown that increasing the effective mass of the carrier increases S but reduces the carrier mobility and hence the electric conductivity σ according to the Eq. (viii). The thermal excitation of carrier from valence band to conduction band creates holes and electrons in case of the narrow semiconductor. However, the concentration of the major carrier does not vary much. Bipolar effects takes place when two types of carriers are present [26] and this is notorious to achieve effective thermoelectrics. The important effect is conduction of the heat from hot side to cold side even during the absent of the net current, the origin of K_{bi}. The next is the suppression of Seebeck coefficient by the presence of both carriers with opposite signs of electronics charge. The K_{bi} for n type materials can be expressed as [27]

$$K_{bipolar} = \sigma_e T \left(\frac{k_B}{e}\right)^2 \left(\frac{(2r+5+\eta_g)^2}{1+e^{\eta_f} e^{\eta_g} \left(m_e^*/m_h^*\right)^{3/2} \left(\mu_e/\mu_h\right)^{3/2}}\right) \quad \text{(ix)}$$

Please cite this article as: H. Alam, S. Ramakrishna, A review on the enhancement of figure of merit from bulk to nano-thermoelectric materials, Nano Energy (2013), http://dx.doi.org/10.1016/j.nanoen.2012.10.005

In short, any attempt to increase σ, will increase K_e which contributes to thermal conductivity (K). In order to counter the increment of K_e, K_{th} can be decreased by various approaches. However, decreasing K_{th} with phonon scattering by adding defects results in decrease in carrier mobility and electrical conductivity. These are the major conflicts in the bulk materials properties which were addressed in the researches for more than a half century. Most of the efforts have been spent on reducing the lattice thermal conductivity by phonon engineering in bulk materials and low dimensional materials [28]. Spitzer reports that for semiconductors, the lower limit for the lattice thermal conductivity is 0.2 W/mK [29]. Due to the lower limit of the K_{th}, there are suggestions to exploit the electronic thermal conductivity rather than K_{th}. The distribution of carriers (of a given energy in the transport process) with zero variance or no spread around the mean value is called Dirac delta distribution. At this narrow band, K_e can be minimized without decreasing the electric conductivity σ. This narrow bands produce high effective masses and hence the large Seebeck coefficient and hence the enhanced power factor [29]. In addition to lowering the thermal conductivity, another criteria to achieve the ZT$\sim$1, the material should be able to attain some minimum values of important parameters such as S$\sim$150 μV/K; no matter if the material possess the lowest thermal lattice conductivity $K_{th}=K_{min}$ [30]. Based on the above explanations, the ideal thermoelectric materials are desired to have the distribution of energy carriers as narrow as possible, the high carrier velocity in the direction of the applied field, and the defects to scatter phonons in order to enhance ZT. However, Pichanusakorn et al. postulates that it is the sheer magnitude not the shape of the DOS that is important [23].

The thermopower (or Seebeck coefficient) is less than the characteristic value 87 μV/K in case of metals. It is very low in the order of 1–10 μV/K for metals and much larger in the order of 10^2 to 10^3 μV/K for semiconductors. The heavily doped semiconductors were found to have comparatively a good ZT. The thermoelectric materials thus comprise of a huge family, including different materials from semimetals, semiconductor to ceramic, containing various crystalline forms from monocrystals, polycrystals to nanocomposite and covering varying dimensions from bulk, film, wire to cluster. Some polymers are also showing interesting thermoelectric material properties recently [31].

Enhancing ZT in bulk materials—alloying and doping approach

Ewing in 1881, studied the effects of mechanical stress on the thermoelectric quality of metals and found that the cyclic phenomenon so conspicuous is not peculiar to the thermoelectric effects of stress, but is probably present in other effects of stress and other parameters such as temperature when this is subjected to increment and decrement [32]. In 1904, there were attempts to study the change of quality of thermoelectric power by magnetization with iron, nickel and cobalt [33]. Anisotropic thermoelectric power in different crystals with deliberately introduced crystal defects with graphites was also explained [34]. Allnatt and Jacobs studied the single crystal pure potassium chloride under 561–963 °C. They also proposed a theory of thermoelectric in 1961[35] and conducted many experiments on some ionic crystals to show potential produced even in the absence of temperature gradient at 470–570 °C [36].

In the other direction, in 1930s, the researchers, gained interests in the synthetic semiconductor based thermoelectric materials having Seebeck co-efficient in excess of 100 μV/K [15]. It was Ioffe who developed the theory of semiconductor, initiated wide research in semiconductors based thermoelectric materials [37]. In the semiconductors, the ratio of thermal conductivity to electrical conductivity (K/σ) was greater than in metals owing to their poorer electrical conductivity. In 1956, Ioffe and coworkers demonstrated that the ratio could be decreased if the thermoelectric material is alloyed with an isomorphous element or compound [38]. The major approach to enhance the thermoelectric properties in bulk materials was carried out by tuning or doping techniques to vary the lattice thermal conductivity without affecting the electrical conductivity. A good thermoelectric material with very high ZT is typically heavily doped semiconductors with low thermal conductivity.

The simple and commonly available thermoelectric material is Bismuth Telluride (Bi_2Te_3) with interesting features of its Seebeck coefficient depending on its composition. An undoped Bi_2Te_3 corresponding to 60 atomic present Te-is p-type with a Seebeck coefficient of about 230 μV/K. As the concentration of Te increases, the Seebeck coefficient gradually falls to zero then changes its sign to become negative (n-type). The maximum ZT of p-type and n-type Bi_2Te_3 crystalline materials (not alloys) at room temperature are about 0.75 and 0.86, respectively [16].

The alloying allows fine tuning of the carrier concentration of the lattice thermal conduction. This does not decrease electric conductivity but lowers only the thermal conductivity. As there is a complete solid solubility among Bi_2Te_3, Sb_2Te_3 and Bi_2Se_3, the addition of Sb_2Te_3 and Bi_2Se_3 to Bi_2Te_3 improves the ZT by reducing lattice thermal conductivity without causing too much degradation of electronic properties. In the low temperature regions, up to 300 K, Bi_2Te_3 and Sb_2Te_3 alloys were found working fine [16,25]. Doping Bi_2Te_3 shifts its properties accordingly. Cs, for example in Bi_2Te_3 material ($CsBi_4Te_6$) exhibits a high thermoelectric ZT below room temperature ($\sim$ 0.8 at 225 K). At cryogenic temperatures, the thermoelectric properties of $CsBi_4Te_6$ are matching with or exceeds that of Bi_2Te_3 [39].

The group IV tellurides (PbTe, GeTe, SiTe) based thermoelectric materials are used at higher temperature around 500–900 K. Both n and p-type PbTe samples can be produced by making PbTe departure from its stoichiometry and by adding some impurities such as chalogenides ($PbCl_2$, $PbBr_2$, PbI_2 etc.) and chalcogenides as donors and alkali metals (Na_2Te, K_2Te etc.) as acceptors. The ZT of PbTe is about 0.001 at room temperature but found surpassing Bi_2Te_3 at higher temperatures. PbTe are usually used by substituting Sn for Pb to form $Pb_{1-x}Sn_xTe$ or Se for Te to form $PbTe_xSe_{1-x}$. While it is possible to obtain a value of ZT slightly above 1 for n-type PbTe alloys at a temperature of about 600 K, the ZT for the p-type PbTe alloys is only about 0.7 [16]. Alloys with $AgSbTe_2$ have stimulated interests in researches to increase ZT$>$1 for both p and n type materials. The p type alloy $(GeTe)_{0.85}(AgSbTe_2)_{0.15}$ known as TAGS, has ZT about 1.2 at around 400 K for long life applications

Please cite this article as: H. Alam, S. Ramakrishna, A review on the enhancement of figure of merit from bulk to nano-thermoelectric materials, Nano Energy (2013), http://dx.doi.org/10.1016/j.nanoen.2012.10.005

[40]. Since telluride is a rare in the Earth's crust (0.001 ppm) even compared to Pt (0.005 ppm) and Au (0.004 ppm), PbSe and PbS were found as an alternative to Te [27]. The traditional semiconductor materials like SiGe alloys (used as high temperature thermoelectric materials) were reported to have low ZT in >900 K due to high thermal conductivity because of their diamond structure [25].

The coexistence of a large thermopower (~100 μV/K at 300 K) and a low resistivity was found in the transition-metal oxide $NaCo_2O_4$ which made this compound an attractive candidate for thermoelectric (TE) application. This compound has two orders of magnitude larger carrier density (~10^{21} cm^{-3}) but showing thermopower comparable to that of the usual low carrier density TE materials [41]. With this the partial replacement of Na with Ca systematically increases the thermopower. This enhancement showed the strong correlation with the electronic specific heat (γ). Though the Ca substitution does not reduce γ, value appreciably, it reduces the carrier concentration and increases thermopower. The Na with Ca substitution (Na, Ca)Co_2O_4 also led a crucial conclusion on low dimensionality of materials (which will be discussed later part this review). The high thermoelectric properties of this material are attributed to the enhanced effective mass coming from entropy of Co^{4+} in the low state spin [42]. Later Fujita et al. reported that ZT of single crystal $NaCo_2O_4$ exceeding 1 at about 1000 K [43] and Ohtaki et al. of ZT 0.8 at 1000 K with polycrystalline $NaCo_2O_4$ [44]. Sugiyama et al. reported that for both Na_xCoO_2 and 3 and 4 layer cobaltides, a common low temperature magnetic state form in the CoO_2 [45].

The above cobalt based oxide semiconductors and their derivatives are p-type semiconductors which have potential advantages over conventional high temperature thermoelectric semiconductors such as SiGe based alloy (ZT~1) and β-$FeSi_2$ (ZT~0.3) in terms of chemical and thermal resistance at around 1000 K. On the other hand n-type semiconductors which are inevitably required as a partner of the p-type oxide semiconductors to develop thermoelectric power generators, have exhibited rather a low ZT values of~0.3 for Al-doped ZnO at 1273 K and ~0.31 for $In_2O_3(ZnO)_m$ (m=integer) at 1073 K. Shingo Ohta et al. developed heavily doped $SrTiO_3$ as a promising candidate for p type semiconductors due its large effective mass (m=6-10 m_0). Also bulk single crystals of heavily La-doped $SrTiO_3$ have been found to have large power factor of 3.6×10^{-3} W/mK^2 at the room temperature which is comparable to that of practical Peltier material Bi_2Te_3 [46]. This research group, in addition to La, used Nb as dopant after solving the issue of solubility of Nb in $SrTiO_3$ lattice.

The compound Zn_4Sb_3 was reported as one of the most efficient thermoelectric materials. Its high efficiency is due the extraordinary low thermal conductivity comparable to that of glass in conjunction with the electronic structure of a heavily doped semiconductor. The thermopower of Zn_4Sb_3 is 13 μW/cmK^2 at 400C which is high but still less than half that of the next best thermoelectric material (AgSbTe2)0.15 (GeTe)0.85 (TAGS) [40]. Jeffrey et al. reported that Zn_4Sb_3 contains significantly glass like interstitial sites, with zinc atoms distributed over multiple positions. This acts as an effective mechanism for lowering thermal conductivity [47].

β-Zn_4Sb_3 has been found to be having thermal conductivity that is nearly independent of temperature between 300 K and 650 K [48]. This is unusual since K_{th} is inversely proportional to T. This also exhibits the value of K_{th}=0.6 W/mK at 300 K which is nearly two fold lower than the Bi_2Te_3 alloys. The Seebeck coefficient too increases with increasing temperature and peaks at 675 K to about 200 μV/K that can be considered to be the best among semimetals. This is one of the best ZT obtained with polycrystalline sample of about 1.3 at 675 K as shown in [48] by 1997. Similar to β-Zn_4Sb_3, $CsFe_{4-x}Co_xSb_{12}$ gives ZT of 1.3 but at 900 K [30]. Further reduction in K_{th} was found with $Zn_{4-x}Cd_xSb_3$ mixed crystals but it is less temperature stable than the β-Zn_4Sb_3. More optimization with these materials seems to be limited considering the doping techniques and the restricted compositional variation possible. However, since 1960s there was no much enhancement of ZT and in the next four decades the research community lost its quest to find new materials. However, there were military and space applications those were giving sufficient but slow momentum.

Cu_2Se is a potentially interesting thermoelectric material which can compete with other conventional TE materials. The ZT of ~1.6 was obtained at 973 K with its β-phase made by ball milling and hot pressing. The disordered Cu atoms were observed to have random motion at high temperature that causes its specific heat abnormally [49]. The resulting thermal conductivity is 0.4–0.5 W/m/K (Fig. 2).

Strategies to enhance ZT with novel approaches

A renewed interest in thermoelectrics began in 1990s after the four decade of slowdown in the research. The novel approaches opened several possibilities to enhance ZT. One of the widely adopted methods to enhance ZT is to reduce the lattice thermal conductivity. Three general approaches are mainly used to reduce the thermal conductivity. In one approach, phonon scattering is used to reduce the thermal conductivity. It can be achieved by scattering phonos in different frequency ranges utilizing a variety of methods such as mass fluctuation scattering (a mixed crystal in ternary and quaternary compounds), grain boundary scattering due to the size of the grains and interface scattering in thin films or multilayer systems.

In the second approach to reduce thermal conductivity, complex crystal structures were used to separate the electron crystal from the phonon glass. In the third method, multiphase composites were mixed on the low dimensional materials to increase scattering [50]. By using heavy masses, with low spring constants and the larger unit cells, lattice thermal conductivity K_{th} was found reduced. In addition to it, K_{th} was reduced by means of solid solution alloying. Complex bulk materials like skutterudites, clathrates and Zintl phases have been explored and reported as one of the several ways to obtain high figure of merits. Many researchers reduced thermal conductivity by creating disorder in unit cells like interstitial sites or partial occupancies in the alloying. For example, rare earth chalcogenides ($La_{3-x}Te_4$) with Th_3P_4 structure have relatively low thermal conductivity due to large number of random vacancies [51]. As phonon scattering by alloying is depending on the mass ratio of the alloy constituent, the random vacancies are found to be ideal scattering sites. The developments in nano-sized structures give new possibilities apart from using complex structures. The transport properties which are

Please cite this article as: H. Alam, S. Ramakrishna, A review on the enhancement of figure of merit from bulk to nano-thermoelectric materials, Nano Energy (2013), http://dx.doi.org/10.1016/j.nanoen.2012.10.005

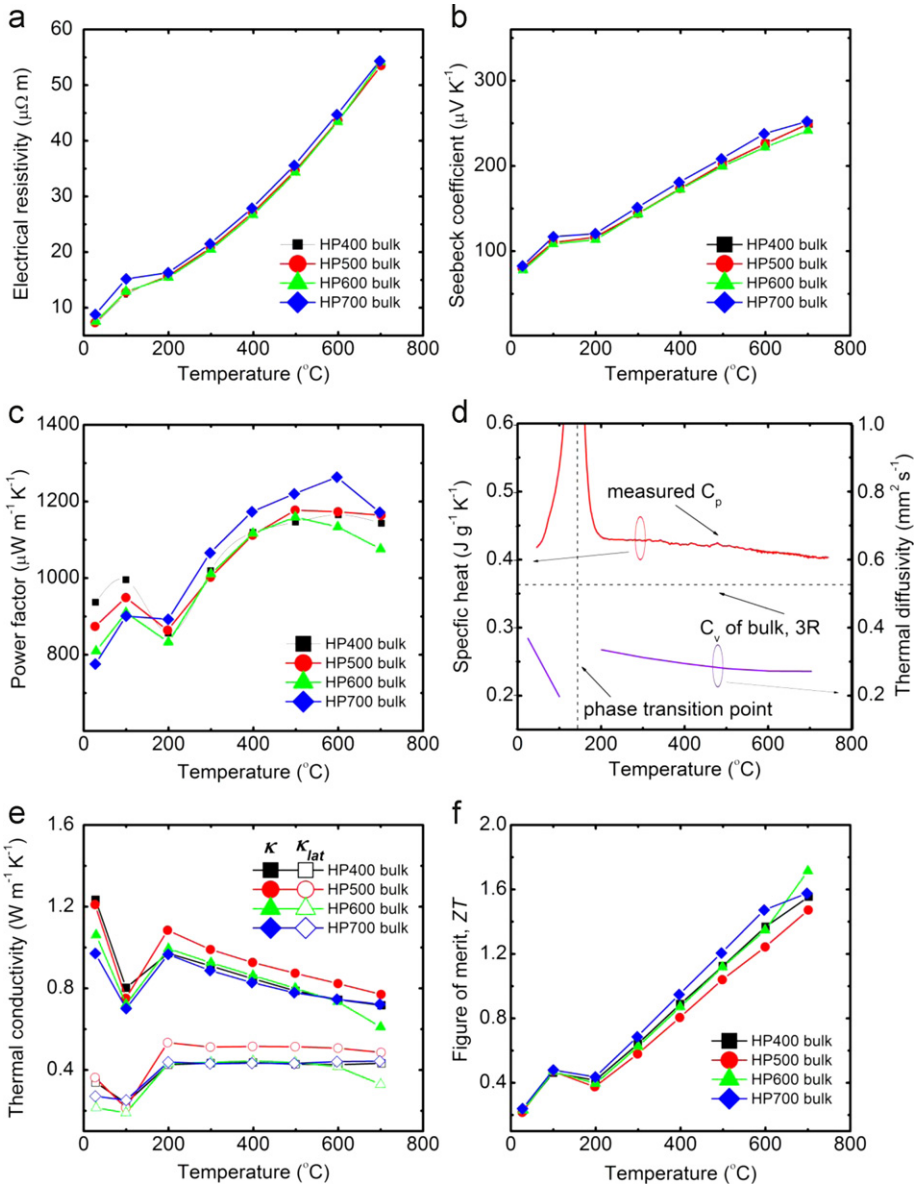

Figure 2 Temperature dependent thermoelectric properties of $Cu_2Se_{1.01}$ bulk samples prepared with different hot pressing temperatures. (a) Electrical resistivity, (b) Seebeck coefficient, (c) power factor, (d) specific heat (Cp), and thermal diffusivity (HP700 bulk), (e) Total thermal conductivity (filled symbols) and lattice thermal conductivity (open symbols) and (f) figure-of-merit, ZT [49].

interrelated in the bulk materials become relatively simpler to handle independently in nanoscale structures. This spurred new interests on the thermoelectric among the researchers to the new height.

Half Heusler materials—mass fluctuation strategy

One of the general strategies to reduce the thermal conductivity is, to introduce the mass fluctuations in the half Heusler materials. The half Heusler materials get their reputation for being high temperature thermoelectric materials owing to their high temperature stability. The structure of half Heusler, generally denoted as ABX, is a simple rock salt structure formed by A and X and filled with element B at one of the two body diagonal positions (1/4, 1/4, 1/4) in the cell, leaving the other one (3/4, 3/4, 3/4) unoccupied [27]. Half Heusler alloys having MgAgAs type crystal structure are forming three interpenetrating face-centered-cubic (fcc) sublattices with one Ni sub-lattice vacant. Despite of having small band gap semiconductors with a gap of 0.1–0.5 eV, high thermopower (S$\sim$ 300 μV/K) and high electric conductivity yielding very high power factors at room temperature, their high thermal conductivity ($\sim$10 W/mK) impose challenges in attaining high ZT [52]. These issues were solved with series of researches by increasing the phonon scattering via chemical substitutions and nanocomposite inclusions.

ZrNiSn being a subset of a much larger family of MgAgAs type structure has a band gaps of about 0.21–0.24 eV [53]. and are known to have a band gap inter-metallic compounds with large thermopower and semi-metallic to semiconducting transport properties. Shen et al. introduced the phonon mass fluctuation scattering by alloying Hf on Zr site that led to an overall reduction of the total thermal conductivity *K*.

Please cite this article as: H. Alam, S. Ramakrishna, A review on the enhancement of figure of merit from bulk to nano-thermoelectric materials, Nano Energy (2013), http://dx.doi.org/10.1016/j.nanoen.2012.10.005

This group explored the effect of less than 1 at% Sb doping on the Sn site, which results in several orders of magnitude lowering of the resistivity without significantly reducing the Seebeck effect and leading to large power factors compared to the state-of-the-art materials. Later Shen et al. explored the effect of isoelectronic alloying of Pd on Ni site, trying to reduce K of these compounds further. As a result of these two, in $Hf_{0.5}Zr_{0.5}Ni_{0.8}Pd_{0.2}Sn_{0.99}Sb_{0.01}$ compound, a power factor of 22.1 $\mu W/K^2cm$ and a thermal conductivity as low as 4.5 W/mK were achieved at the room temperature. The ZT increased to 0.7 with the increment of temperature to 800 K.

Browning et al. reported that even though the properties of ZrNiSn compound varied greatly with various chemical substitutions, no net increase in ZT was achieved. However, Uher et al. suggested the substitution of Indium samples in ZrNiSn compounds to enhance ZT. The preliminary measurement of chemically substituted TiNiSn suggested that this system may hold promise for enhanced ZT values in chemically disordered materials [54].

Hiroaki Muta et al. applied substitutions and additions of the excess nickel to ZrNiSn compounds and conducted experiments from the room temperature to 1000 K. The lattice thermal conductivity of $Zr_{0.7\times0.3}NiSn$ (X=Ti, Hf), $ZrNi_{0.7}Y_{0.3}Sn$ (Y=Pd, Pt) and $ZrNi_{1.05}Sn$ compounds were determined and found that the excess amount of nickel caused a drastic reduction of the lattice thermal conductivity up to 700 K. Beyond that limit, it started increasing due to ambipolar effect which depends on the hole transport properties. It indicates the necessity to disturb the hole conduction (or electronics conduction as a p type materials) for reduction of the additional electronic thermal conduction. $Ti_{0.5}Zr_{0.25}Hf_{0.25}NiSn$ was reported to have very large ZT=1.5 at 700 K. The alloying Hafnium together with titanium resulted in a strong reduction of the thermal conductivity [55]. Thermoelectric properties of ZrNiSn was attempted to improve by changing the degree of antisite defects of Zr and Sn atoms Qiu et al. [56]. These antisites are found to shrink the band gap combined with the enhanced DOS slope contributing to the improved electrical transport properties. As a result, a high ZT of 0.64 at 800 K was attained without doping or isoelectronic alloying. While many n type half Heusler compounds have been investigated on their high temperature thermoelectric properties, only a very few high temperature p type half Heusler compounds such as ZrPtSn, HfPtSn, ErPdSb and ErPdBi have been reported.

Another interesting half heusler material TiCoSb is sensitive to the Ti and Co sites due to the conduction band and the valence band of TiCoSb compound that consist of 3d orbitals of Ti and co atoms. TiCoSb has an energy band gap of 0.95 eV which is the highest among the half Heusler compounds. Sekimoto et al. prepared (Ti, Zr, Hf)CoSb systems by arc melting method and obtained ZT of 0.025 on TiCoSb at 921 K [57]. Including Fe, in p type $TiFe_xCo_{1-x}Sb$, with randomly distributed TiO_2 increases the electrical conductivity. It causes the increment of the Seebeck Coefficient to 300 $\mu V/K$ at 850 K for x=0.15. With the inclusion of a small amount of Fe, TiCoSb shifts from n type to p type conduction. Increasing Fe causes the drastic reduction of thermal conductivity due to the presence of TiO_2. The mass fluctuation and strain field fluctuation due to the substitution of Fe to Co site too contributes the reduction in thermal lattice conduction. Comparing to the state of the art materials, the thermal conductivity is still high to 3.7 W/mK at 850 K. The ZT is 0.45 for $TiFe_{0.15}Co_{0.85}Sb$ which is relatively higher among p type half Heusler [58]. Wu et al. [59] doped Ge in TiCoSb compounds and found the increment of Seebeck Coefficient, electrical conductivity with the increasing Ge. The Seebeck coefficient changed from negative to positive with Ge doping at 850 K. Interestingly, the thermal conductivity reduced considerably because the point defect induced by Ge substitution for Sb intensively scatters the phonons. The reduction of the lattice thermal conductivity is mainly attributed to the strain field fluctuation. However, the thermal conductivity was still higher than the state of the art materials. The ZT of $TiCoGe_{0.15}Sb_{0.85}$ was found to be 0.16 at 850 K.

Qiu et al. [60] achieved a decent ZT in TiCoSb compounds by alloying Zr on the Ti site. In this alloy, the electronics conductivity and thermal conductivity were suppressed while the Seebeck coefficient was improved dramatically with the highest value of -420 uV/K for $Ti_{0.5}Zr_{0.5}CoSb$ at 600 K. This provides a large space for optimizing the thermoelectric performance. Also by doping Ni on the Co site resulted in increasing the electrical conductivity remarkably with the still large Seebeck coefficient. The ZT of 0.7 at 900 K was achieved for $Ti_{0.6}Hf_{0.4}Co_{0.87}Ni_{0.13}Sb$.

Sekimoto et al. studied the properties of polycrystalline sample of XPdBi (X=La, Gd). The band gap of LaPdBi and GdPdBi were found to be 0.05 and 0.07 eV, respectively, and showed the semiconductor like behavior with the electrical resistivity of $10^{-6}\,\Omega$ m. Increasing the temperature increases the carrier contribution on the electronic thermal conductivity and decreases its positive thermopower. The maximum ZT for LdPdBi at 615 K was just 0.085 and for GdPdBi at 469 K was just 0.084 [61] (Table 1).

XCoSb as p type materials and XNiSn as n-type materials have been used in most of the researches (X=Ti, Zr and Hf) [62]. While XNiSn compounds have high ZT, the ZT of the ACoSb compounds were less comparing its counterpart. Wang et al. reported the computational model with the electronics properties with Pseudopotential and Korringa-Kohn-Rostoker methods to explore the ways to enhance the thermoelectric properties of half Heusler materials [62]. Apart from (Ti, Zr, Hf) CoSb, (Ti, Zr, Hf) NiSn, (V, Nb, Ta)CoSn there are less investigated half Heusler materials such as NbCoSn, NbRhSn, ZrCoBi, VFeSb, NbFeSb for p type and LaPdBi, NdCoSn, YNiSb, ZrCoBi for n type materials [27]. Generally arc melting and spark plasma sintering methods are widely adopted for preparation of half Heusler materials.

Complex cell structures—clathrates, skutterudites and Zintl phase with rattling strategy

Slack suggested a new criterion for finding better thermoelectrics in which the cage compounds with a large unit cells containing encapsulated atoms that can ''rattle'' inside the voids will have a low thermal conductivity [63]. The problem in skutterudites or clathrates is high thermal conductivity due to strong bonding and simple order, and this was solved by doping carrier concentration for electron-

Please cite this article as: H. Alam, S. Ramakrishna, A review on the enhancement of figure of merit from bulk to nano-thermoelectric materials, Nano Energy (2013), http://dx.doi.org/10.1016/j.nanoen.2012.10.005

Table 1 Figure of merits of half Heuslers materials of NiSn, CoSb and PdBi groups with substitutions such as Ti, Zr, Hf, La and Gd. NiSn groups shows promising performance with Ti, Zr and Hf substitutions. Most of the half Heuslers materials are used for high temperature applications.

Compounds	Substitutions	*ZT*	Temperature (K)
XNiSn (X=Ti, Zr and Hf)			
$Ti_{0.5}Zr_{0.25}Hf_{0.25}NiSn$ [55]	Ti/ Hf	1.5	700
ZrNiSn [56]	Antisites	0.64	800
$Hf_{0.5}Zr_{0.5}Ni_{0.8}Pd_{0.2}Sn_{0.99}Sb_{0.01}$ [53]	Pd on Ni	0.7	800
XCoSb (X=Ti, Zr and Hf)			
TiCoSb [57]	Ti	0.025	921
$TiFe_{0.15}Co_{0.85}Sb$ [58]	Fe on Co	0.45	850
$TiCoGe_{0.15}Sb_{0.85}$ [59]	Ge on Sb	0.16	850
$Ti_{0.5}Zr_{0.5}CoSb$ [60]	Zr on Ti	NA	600
$Ti_{0.6}Hf_{0.4}Co_{0.87}Ni_{0.13}Sb$ [61]	Ni on Co	0.7	900
XPdBi (X=La, Gd)			
LdPdBi [61]	-	0.085	615
GdPdBi [61]	-	0.084	496

phonon interaction. In addition to it, alloying with transition metals or antimony sites reduces thermal conductivity. The size and vibrational motion of the filling atoms and the thermal conductivity leads ZT to as high as 1. Also rare earth or other heavy atoms can fill the voids leading to lower the thermal conductivity. Large space for the filling atoms in the skutterudites or clathrates cause soft phonon modes and rattling mode that reduces thermal conductivity.

Bulk materials such as Bi_2Te_3 can be further modified with complex variants. $CsBi_4Te_6$ is for example a complex variant of commonly used Bi_2Te_3 and it has lower thermal conductivity than Bi_2Te_3. Cs adds complexity with Cs layers and Bi-Bi bonds. The Bi-Bi bonds lowers the band gap and this shifts the peak ZT of 0.8 to lower temperature than that of Bi_2Te_3. $CsBi_4Te_6$ has also anisotropic effective mass which improve Seebeck co-efficient with slight detriment of mobility [64]. Many ordered MTe/ Bi_2Te_3 type variants (*M*=Ge, Sn or Pb) are known making up a large homologous series of compounds with $Zt=0.6$. Many of these materials are still not explored well with doping. Low thermal conductivity can be obtained with thallium based thermoelectric materials such as Ag_3TlTe_3 and Tl_9BiTe_6. Apart from complex unit cell, the unique property of thallium of being extremely soft bonding leads to the low thermal conductivity (0.23 W/mK at room temperature) [65].

Clathrates are one of the new classes of candidates with tetrahedrally coordinated atoms forming a cage around a metal atom. The general formula of type I clathrates is $A_xB_yC_{46-y}$. The B and C are tetrahedrally bonded to make a framework that forms cages around the guest atom A. A_8C_{46} (with *A*=Na, K, Rb; *C*=Si, Ge, Sn), $A_8B_8C_{38}$ (with *A*=Na, K, Rb; B=Al, Ga, In; *C*=Si, Ge, Sn) and $A_8B_{16}C_{30}$ (with *A*=Sr, Ba, Ca; B=Al, Ga, In; *C*=Si, Ge, Sn) are example of clathrates candidates. In these compounds the anionic frameworks are covalently bonded providing them a medium for high carrier mobility [66]. Usually type I clathrates compounds consist of two pentagonal dodecahedra (X_{20}) and six tetrakaidecahedra (X_{24}) in the cubic unit cell of the space group of Pm3n [67] as shown in the Fig. 3.

$Sr_8Ga_{16}Ge_{30}$ is one of the most interesting clathrates exhibiting n-type semiconducting behavior with four

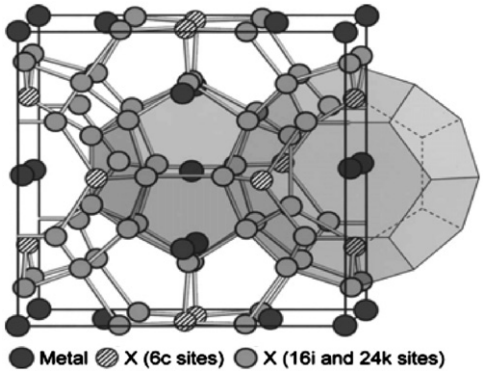

Figure 3 Crystal structure of type-I clathrate compounds. A dodecahedron (X_{20}) centered at the body center of the unit cell and one of its neighboring tetrakaidekahedra (X_{24}) are indicated in the figure. The atoms in the 6c sites are indicated with shaded circles.

cornered diamond lattice structure of Ge with Sr inside the cage. It is common to assume that the metal atoms inside the cage donate electrons to the frame which causes the rattling ions scattering conduction electrons, lowering the conductivity. This would be a harmful effect if the electrical conductivity were to take place through Sr. If Sr is ionized, the $Sr_8Ga_{16}Ge_{30}$ is not a PGEC material. However, the experimental result of $Sr_8Ga_{16}Ge_{30}$ shows the high Seebeck coefficient $S=-320\,\mu V/K$ with low thermal conductivity $K=0.9$ W/mK at the room temperature [68]. This shows $Sr_8Ga_{16}Ge_{30}$ closer to being PGEC material than the common opinions. Bo B Iversen showed that Sr atoms in the clathrates are practically neutral, that Sr is weakly bound to the cages and rattle around, that the electrical conductivity takes place through the frame, and that Sr-based bands do not contribute to the transport coefficient [69]. Even though $Sr_8Ga_{16}Ge_{30}$ is a metal, it has high Seebeck coefficient because of its sharp peak in the density of states at the Fermi level, which is known to lead to a large Seebeck coefficient. The high density of states leads to an increase

Please cite this article as: H. Alam, S. Ramakrishna, A review on the enhancement of figure of merit from bulk to nano-thermoelectric materials, Nano Energy (2013), http://dx.doi.org/10.1016/j.nanoen.2012.10.005

of the electronics contribution to the thermal conductivity. The carrier concentration is reported to be around10^{17}-10^{19} cm^{-3} [70].

Some type I clathrates such as Ba_8Ge_{43}, K_8Ge_{44}, $(K,Cs)_8Sn_{44}$ and Rb_8Sn_{44} are reported to have chemical composition deviated from the general formula A_8C_{46}. While one-third of the 6C sites for X atoms are found to be randomly distributed for K_8Ge_{44}, $(K,Cs)_8Sn_{44}$ and Rb_8Sn_{44}, half the 6C sites for Ge atoms are occupied in an ordered manner in Ba_8Ge_{43} [67]. Hermann attributed the additional reflection to the ordering of Ge vacancies in the 6C sites. However, its ZT was measured to be very low value of 0.057 [71]. It changes from Ba_8Ge_{43} superlattice structure to normal Ba-Ga-Ge type I clathrates structure when Ga content is increased. The density of Ge vacancies decreases with the Ga contents and this results in increasing Seebeck coefficient, electrical conductivity while reduction of lattice thermal conductivity. [72].

Beintien et al. showed with $Ba_8Ga_{16}Ge_{30}$ the single crystalline samples that the excess of Ga shifted it to p-type semiconductor and thermal conductivity similar to iso structural $Eu_8Ga_{16}Ge_{30}$ and $Sr_8Ga_{16}Ge_{30}$ [73]. Hou et al. grew $Ba_8Ga_{16}Ge_{30}$ clathrates by the Czochralski methods and investigated with varied ratios of Ga/Ge [74]. The lower pulling and higher pressure resulted in larger Ga/Ge ratio and crystal was found homogeneous. They showed the larger electrical conductivity and lower thermal conductivity with higher Ga/Ge ratio which does not affect the Seebeck coefficient. They obtained ZT $Ba_8Ga_{16}Ge_{30}$ 0.93 at 850 K and 1.3 at 1000 K. The loss of Ga during heat treatment above certain temperature like 600 °C resulted in shifting from p type to n type extrinsic semiconductor and showed high thermal power and reduced electrical conductivity. After heat treating at 800C, the crystal structure seemingly loses less Ga and has negative impact on ZT [75]. However, the change of Ga/Ge ratios in $Sr_8Ga_{16}Ge_{30}$ was reported to be working on the other way. The electrical conductivity was found to be increasing and the Seebeck coefficient decreasing with decreasing Ga/Ge ratio. The thermal conductivity was maintained at the same order lower than 1 W/mK at the room temperature and ZT was obtained as 0.85 at 650 K for the lowest Ga/Ge ratio sample of $Sr_{16.86}Ga_{27.01}Ge_{56.13}$ [76].

Hokazono et al. attempted to increase the Hall mobility in the $Ba_8Ga_{16}Ge_{30}$ material by substituting Ga with Cu. He obtained the Hall concentration in n type $Ba_8Cu_xGa_yGe_{46-x-y}$ in the order of 10^{-20}/cm that is comparable with type VIII $Ba_8Ga_{16}Ge_{30}$ stoichiometric compounds. The Seebeck coefficient was maintained to the higher value due to the higher effective mass of the conduction band similar to the value of n type $Ba_8Ga_{16}Ge_{30}$. The inverse temperature dependance of the Hall mobility indicates the main scattering mechanism of conduction electrons is alloy disorder scattering in the temperature range of 80 to 300 K [77]. Eto et al. took on extensive studies on the band gap of intrinsic semiconductor $Ba_8Zn_xGe_{46-x}$ which possess indirect band gap and compared with that of $Ba_8Zn_8Ge_{38}$ the n type degenerate semiconductor and $Ba_8Zn_{10}Ge_{36}$ the p type degenerate semiconductor by substituting Zn with Ga. $Ba_8Zn_6Ga_4Ge_{36}$ was reported to have Eg=0.9 eV which is wider than that of $Ba_8Zn_8Ge_{38}$ (Eg=0.4 eV) and better thermoelectric characteristics than $Ba_8Zn_8Ge_{38}$ at high temperature [78].

The p-type group IV clathrates Ba_8MGe_{40} (M=Cu, Ag, Au) were found to have narrow band gap because of noble metal doping. The thermoelectric power increases with temperatures monotonically and magnitude was found to be smaller than 100 mV/K at 1000 K [79]. The detailed study was made by Falmbigl et al. with $Ba_8N_xGe_{46-x}$ and $Ba_8N_xSi_{46-x}$ (N=Cu, Zn, Pd, Ag, Cd, Pt and Au) and listed in [80].

Another impressive work from S Deng et al. shows the substitution of Al for Ga in $Ba_8Ga_{16}Sn_{30}$ material increases the negative Seebeck coefficient (300 uV/K at 600 K) due to its metallic behavior in electrical resistivity. Known as type VIII clathrates $Ba_8Al_xGa_{16-x}Sn_{30}$ its ZT reaches 1.2 at 500 K when x reaches 6 [81]. The authors suggest the possible further improvements by controlling the starting compositions of Al and Sn. The recent similar work on $Ba_8Ga_{16}Sn_{30}$ in which Cu replaces Ga shows that the ZT for x=0.033 reaches the maximum of 1.35 at 540 K [82].

Mudryk et al. prepared a novel europium substituted clathrates, $Eu_{2-x}(Sr,Ba)_{6-x}$ M_y Si_{46-x} (M=Al, Ga) that are consistent with type I clathrates. Eu atoms occupy Ba compounds preferentially the 2a position and thus form a new quaternary version of the $Ba_8Al_{16}Ge_{30}$ structure type. The researchers found that $Eu_2Ba_6Al_8Si_{36}$ and $Eu_2Ba_6Ga_8Si_{36}$ exhibit long-range magnetic order below 32 and 38 K of presumably ferromagnetic type. Because of the low thermopower in the order of 100uV/K, the ZT was achieved as 0.025 only for $Ba_8Al_{16}Si_{30}$ [83].

Nolas et al. investigated the transport properties of several Sn clathrates with type I hydrate crystal structures such as Cs_8Sn_{44}, $Cs_8Zn_4Sn_{42}$, $Rb_8Zn_4Sn_{42}$, $Rb_8Ga_8Sn_{38}$ and found the low thermal conductivity attributed to the localized disorder associated with the dynamics motion of the alkali metal atoms [84]. Chen et al. investigated the properties of Sn clathrates under hydrostatic pressure and reported some interesting facts of temperature dependence of electrical resistivity and Seebeck coefficient [85]. The theoretical calculation of Sn_{46} shows that the energy gap closes under pressure. The similar effect in Cs_8Sn_{44} and change of semiconductor to semimetal transition are expected. An irreversible increase in Seebeck coefficient was observed in both Cs_8Sn_{44} and $Cs_8Zn_4Sn_{42}$ after application of pressure. This result demonstrates that the power factor can be increased permanently by application of high pressure and suggests the possibility of higher efficiency thermoelectric device. Zaikina et al. investigated thermoelectric properties on $Sn_{24}P_{19.3(2)}Br_xI_{8-x}$ and $Sn_{24}P_{19.3(2)}Cl_yI_{8-y}$ and found $Sn_{24}P_{19.3(2)}Br_xI_{8-x}$ (x=0-8) to be with low band gap value of 0.03 eV to 0.14 eV with linear function of the guest halogen atom ratios. The one of the lowest value of thermal conductivity 0.5 W/mK at the room temperature has been observed for $Sn_{24}P_{19.3}Br_2I_6$. The authors report the lowest degree of ordering of the guest ions leads the significant low thermal conductivity not the rattling of guest atom [86].

Only type I clathrates was relatively well studied while clathrates type II generally ignored due to the difficulty to synthesize it as pure phase with defined components and in a rational and reproducible way [87]. (Cs or $Rb)_8Na_{16}$ (Si or $Ge)_{136}$ was prepared in the pure form in 1999. $Cs_8Na_{16}Si_{136}$, $Rb_8Na_{16}Si_{136}$, $Cs_8Na_{16}Ge_{136}$ and $Cs_8Na_{16}Ge_{136}$ were analyzed and reported along with electrical and thermal transport properties. Type I clathrates are found to have edge over type II clathrates in terms of thermal conductivity especially [88].

Please cite this article as: H. Alam, S. Ramakrishna, A review on the enhancement of figure of merit from bulk to nano-thermoelectric materials, Nano Energy (2013), http://dx.doi.org/10.1016/j.nanoen.2012.10.005

Skutterudites is a cubic structure containing generally 32 atoms per unit cubic cell (Fig. 4). It belongs to the binary semiconducting compounds forming the skutterudites structures consists of CoP_3, $CoAs_3$, $CoSb_3$, RhP_3, $RhAs_3$, $RhSb_3$, IrP_3, $IrAs_3$ and $IrSb_3$. Unlike clathrates, it possesses voids in the structure whether or not guest atoms are present. With the low electronegativity differences such as CoSb3 and Ir Sb3, there is a high degree of covalent bonding enabling high carrier mobilities and hence good electron-crystal properties. The strong bonding and simple order cause to high thermal conductivity and hence the challenge with skutterudites is in reducing the lattice thermal conductivity. Doping the materials to cause rattle reduces the thermal conductivity. In order to maintain the structural stability, filling the skutterudites with electropositive ions in the void with the replacement of the electron deficient neighbor is important [89].

The atomic displacement of La in lanthanum triiron cobalt dodecaantimonide was studied and found that La was too small to fill in the cage. Site occupancy refinements show about 25% vacancies on the La site and an actual Fe:Co ratio of 2.17:1 in $LaFe_3CoSb_{12}$. La atoms are linked to the dramatic decrease of the lattice contribution to the thermal conductivity [90]. Since Ce was thermodynamically stable it was included in $CoSb_3$. Ce and Fe were used in $CoSb_3$ to form $CeFe_3CoSb_{12}$ and found the increased Seebeck coefficient, decreased thermal conductivity in the range of 300 –850 K. The highest ZT of 0.63 was obtained at 700 K [91]. With Ru and Rh, an n type $Ce(Ru_{0.67}Rh_{0.33})_4Sb_{12}$ was prepared under pressure and various temperature in pursuit of excellent ZT and low thermal conductivity. It transformed into p type at 6 GPa and about 700C [92]. The broad range of resonant phonon scattering can be obtained with double filled skutterudites in $CoSb_3$. Ba and Yb fill to form $Ba_xYb_yCo_4Sb_{12}$. The ZT of n type $Ba_xYb_yCo_4Sb_{12}$ was achieved to be 1.36 at 800 K [93],[94]. Bai et al. investigated further with other rare earth materials such as Ce, Yb and Eu in addition to Yb [95].

$Sn_zCo_4Sb_{11.2}Te_{0.8}$ was examined with varied temperature from 300 K to 700 K. Sn filled and Te doped $CoSb_3$ showed n type conductivity at all temperature. In this case Te acts as electron donor by substituting Sb atoms. The ZT was found to be increasing to 0.6 at 700 K and when ZT reached above 2 the ZT started declining due to higher thermal conductivity and electrical resistivity [96]. In filled and Ni doped $CoSb_3$ was synthesized and examined in the range of 300–700 K. The in filling and Ni doping lowered the thermal conductivity and increased optimized carrier concentration. The ZT of $In_{0.25}Co_{3.9}Ni_{0.1}Sb_{12}$ was obtained as 0.9 at 700 K [97]. Multiple filled skutterudites were prepared with Ba, La and Yb $CoSb_3$ and found have achieved ZT of 1.7 at 850 K with $Ba_{0.08}La_{0.05}Yb_{0.04}Co_4Sb_{12}$ [98].

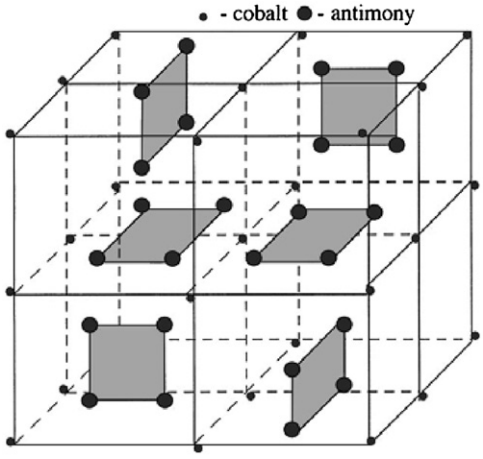

Figure 4 Schematic illustrating the unit cell of the unfilled skutterudite crystal structure.

In addition to the voids, adding ions increases electrons to compensate cations elsewhere in the structure for charge balance and create additional source of lattice disorder. For the case of $CoSb_3$, Fe^{2+} can replace Co^{3+} partially. Similar charge balance can be introduced for clathrates where filling needs replacing group IV (Si, Ge) with group III (Al, Ga) [25]. A *Zintl Phase* compound contains a valance-balanced combination of both ionically and covalently bonded atoms. The ionic cations donate electrons to the covalently bound anionic species. $Yb_{14}MnSb_{11}$ is one such example for the complex Zintl compounds with ZT=1 at 900 K [25].

Enhancing ZT-substructure approach

Substructure approach where distinct regions provide different functions is one of the effective approaches to circumvent the PGEC conflicts. For example, free charge carriers confined to planar Cu–O sheets, are separated by insulating oxide layers. The insulating layers act as charge reservoir that accommodates dopant atoms those donate charge carriers to the Cu–O layers. This separation of the doping and conducting regions keep the charge carriers sufficiently screened from the dopant atoms so as not to trap carriers which will lead to low mobility. The phonon glass regions house the dopants and disordered structures without disturbing the electron crystal regions. The electron crystal regions are needed to be thin on the nanometer or angstrom scale so that phonon of short mean-free path are scattered at phonon glass regions. This thin electron crystal region takes advantage of quantum confinement and/ or electron filtering to enhance Seebeck co-efficient. The skutterudites and clathrates are 0 dimensional version of substructures. Another widely known materials that uses substructure is cobaltite oxides (Na_xCoO_2) and Ca–Co–O[41]. Yang Wang et al. showed the noticeable influences of Ln ion in $[Ca_2CoO_3]_{0.62}[CoO_2]$. The Ln^{3+} changes the hole concentrations and introduces a strong point defect phonon scattering [99].

The CaYbZnSb the Zintl phase compound is similar to Na_xCo_2O with sheets of disordered cations between the layers of covalently bound Zn–Sb and the substructure approach can be clearly seen in it [41,42]. $Ca_xYb_{1-x}Zn_2Sb_2$ is found as promising materials for the thermoelectric applications. It is simple tunability of their transport properties lead to the low carrier concentration from 15 to $3.1 \times 10^{19}/cm^3$ [100]. However its thermal conductivity is very high to ~1.5 W/mK [25]. With the broad range of phonons involved in the heat transportation, long wavelength phonons need disorder on longer length-scales, leading to a need for hierarchal complexity. Combing the substructure approach with nanostructured materials seems to be promising in enhancing the figure of merits.

Please cite this article as: H. Alam, S. Ramakrishna, A review on the enhancement of figure of merit from bulk to nano-thermoelectric materials, Nano Energy (2013), http://dx.doi.org/10.1016/j.nanoen.2012.10.005

Nanostructured thermoelectric materials

Low dimensional materials were used either to enhance the power factor or to reduce the lattice thermal conductivity. In one approach the nanoscale constituents are used to introduce the quantum confinement effects to increase power factors. In the second approach the nanostructures introduce many internal interfaces to scatter phonons. The enhancement of the density of states near E_f leads to the higher Seebeck coefficient. With low dimensional materials it is advantageous with anisotropic Fermi surfaces in multi valley cubic semiconductor and increased mobilities at a given carrier concentration when the quantum confinements are satisfied so that modulation doping and delta doping can be utilized. Thus they give us freehand to manipulate the thermoelectric parameters. The another aspect is that the low dimensional particles are promising candidates in increasing ZT also because Wiedmann Franz law is not applicable to nanomaterials with delta like DOS [101]. The carrier mobility μ is independent of electron-phonon coupling under the normal condition such as near and above the room temperature [102]. Hence phonon drag has been ignored in the most of the calculation in these temperature regions [103].

The theoretical predictions on the strong enhancement of ZT was based on the modification of K_e and power factor due to the spatial confinement of carriers and corresponding change in carrier density of states. These predictions generally ignored spatial confinement of phonon and used bulk values of K_{ph}. It should be noted that even in the superlattices of similar materials, the phonon transport can be modified due to mini-band formation and the emergence of mini-Umklapp processes. The phonon confinement affects the entire phonon relaxation rate and this makes difference in the thermal transport properties of nanostructures from the bulk structures. The simulation results made on Bi_2Te_3 sandwiched between air and soft polymer shows the effect of phonon spatial confinement on thermoelectric properties. The change of phonon group velocities and dispersion due to the spatial confinement leads to the increase of the phonon relaxation rate and strong drop in lattice thermal conductivity. The ZT was simulated to show more increase than its bulk/ ingot counterpart at this condition [103].

2D multiple quantum well (MQW) structures were considered to increase ZT over their bulk counterparts when the quantum well width is reduced. It is mainly because of the density of electron states per unit volume that occurs in the quantum well. PbTe/ $Pb_{1-x}Eu_xTe$ were investigated because of its well established fabrication techniques and its good thermoelectric properties. PbTe/ $Pb_{1-x}Eu_xTe$ MQW samples were grown by Molecular Beam Epitaxy(MBE) with widths varying between 17 and 55 A for x=0.073. The increment of ZT of 2.0 at 300 K occurred only in quantum well due to the enhanced power factor. The lattice thermal conductivity was assumed to be unchanged [104] from its bulk counterparts whose value is below 2 $\mu V^2/K^2cm^3$. Similarly Si/SiGe superlattice systems were studied and increase in power factor was predicted [105]. Ga, In and Tl create additional energy level known as resonant levels in the classical semiconductor PbTe. The ZT has been reported to be doubled in diluted alloys of p type PbTe to 1.5 at 773 K from 1 to 2 atomic % Tl (Tl-PbTe) [106]. The origin of the Tl induced state is still under investigation but ascribed to either valance fluctuation or a hybridization between excited state of group III atom and neighboring Te p-states or additional piece of Fermi level.

While one research group studied 2D superlattice systems in more details to enhance ZT, there were other groups working on the development of the higher whole superlattice sample (denoted as $Z_{3D}T$). The quantum well width and barrier width of GaAs/ AlAs whole superlattice was predicted to have higher ZT than its GaAs bulk values [105].

In addition, the *carrier pocket engineering* (CPE) can improve power factor while the band discontinuities can trap cold electrons in wells to increase the Seebeck coefficient [50]. With Carrier Pocket Engineering, it was calculated that width of quantum well and barrier can be adjusted to raise the energy of lowest Γ point sub-band to higher than the L and X point sub-bands. This increases the density of state for L and X point sub-bands and thereby enhancing $Z_{3D}T$. The calculated value of ZT of GaAs/ AlAs was 0.41 (at the room temperature) which was 50 times higher than that of GaAs value [107]. While the experimental results showed the enhancement of $Z_{3D}T$, the power factor of several superlattices did not show the enhancement of quantum carrier confinement effects including Bi_2Te_3/ Bi_2Se_3, PbTe/ $Pb_{1-x}Eu_xTe$ and Si/SiGe [105].

Energy barrier filtering and high electron density in metal produce large moment of differential conductivity about the Fermi level. Also high interface density, large mismatch in phonon density of states and electron-phonon interface resistance suppress thermal conductivity. If nanoscale roughness can be designed to overcome the constraints of parallel momentum conservation, very high ZT may be possible [108].

The large anisotropy of three ellipsoidal constant energy surfaces for electrons at the L point in the rhombohedral Brillouin zone, the long mean free path of L point electrons and high mobility of the carriers make Bismuth attractive for low dimensional thermoelectric behavior. The decreased quantum well width raise the lowest bound state to the highest bound state in the valence band leading to *semimetal to semiconductor* transition (Fig. 5). The reduction of well width in 2D (quantum dots) and 1D (nanowire) enhances the ZT to above 2 and 6 theoretically [105].

One anisotropic hole pocket at the T point of the Brillouin zone and three highly anisotropic and non-parabolic electron ellipsoids at the L points of Bi nanowire were theoretically studied and attributed that its small effective mass and anisotropic Fermi surface with its peaked DOS. It was found the $Z_{1D}T$ can be achieved if the T point hole can be removed or suppressed to lie below the L point holes. This can be achieved by alloying Bi with Sb to form $Bi_{1-x}Sb_x$ ($0.07<x<0.18$) [109]. The size effect (Fig. 5) was intensively studied on the bismuth nanowires prepared in porous templates and was suggested the smaller nanowires for the enhanced transport properties [110]. (Note: Bi nanowires are chemically unstable with have low melting point of $-271\ ^\circ C$ and hence fabrication and electrical measurements are very challenging)

In the second approach the lattice thermal conductivity is reduced. The finite acoustic mismatch between structure and barrier materials in low dimensional structures leads to the acoustic confinement and corresponding reduction of lattice thermal conductivity in-plane. [111].

Bi_xTe_{1-x} nanowires deposited in the nanopores of anodized alumina membranes using an electrochemical deposition

Please cite this article as: H. Alam, S. Ramakrishna, A review on the enhancement of figure of merit from bulk to nano-thermoelectric materials, Nano Energy (2013), http://dx.doi.org/10.1016/j.nanoen.2012.10.005

method were studied for various ratios. The Seebeck coefficient was found to increase by 15%–60% more than the bulk at 300 K when x=0.46. For higher value of x=~(−0.54), S decreased smaller than the bulk. The surface roughness (r) on order of 1 nm of the nanowire played a crucial role in reducing lattice thermal conductivity without affecting the electron conductivity much as the wavelength of phonon is below 1 nm while the electron's is around 10 nm [112]. Yet the fundamental reasons why and how nano-structuring reduces thermal conductivity in crystalline materials are not fully understood. Kesker et al. recently presented evidence of a significant enhancement of ZT with Bismuth nanotubes and nanowires made by aqueous chemical method and found the thermal conductivity being 5 times less than that of Bismuth powder. The low thermal conductivity is attributed to the reduced lattice thermal conductivity of nanostructured bismuth networks via interface scattering [113]. The ZT increases dramatically to 0.2 at 280 K which is much higher that its powder form as shown in the Fig. 6.

The thermal conductivity of pressure sintered $Si_{0.8}Ge_{0.2}$ alloy is less than that of crystalline alloy because of the heavy point defects. However ZT was not increased due to the proportional reduction of electrical conductivity. Similar results were obtained with Si/Ge superlattice, $Si_yGe_{1-y}/Si_xGe_{1-x}$ superlattice where the reduction of thermal conductivity did not increase the ZT [114]. In GaAs/ AlAs superlattice of the order of 1–4 nm period thickness, the cross-plane thermal conductivity was found less than that of $Al_{0.5}Ga_{0.5}As$ alloy. Bi2Te3/ Sb2Te3 superlattices of 1–5 nm was reported to have less cross-plane thermal conductivity than that of a solid solution alloy [115]. Taking cue from this, Kim et al. embedded ErAs nanoparticles epitaxially into $In_{0.53}Ga_{0.47}As$ as matrix and random manner to compare the results. The ErAs in $In_{0.53}Ga_{0.47}As$ was reported to have increased the electronic thermal conductivity but decreased the phonon contribution due to electron–phonon scattering and phonon scattering [116]. ErAs was reported to give an additional scattering mechanism for mid to long wavelength phonon.

Yan et al. [117] decreased the average grain size to 1 μm in p-type *half Heusler* samples and obtained a slightly enhanced ZT. By reducing the average grain size further to 200 nm $Zr_{0.5}Hf_{0.5}CoSb_{0.8}Sn_{0.2}$ by ball milling the alloyed ingot into

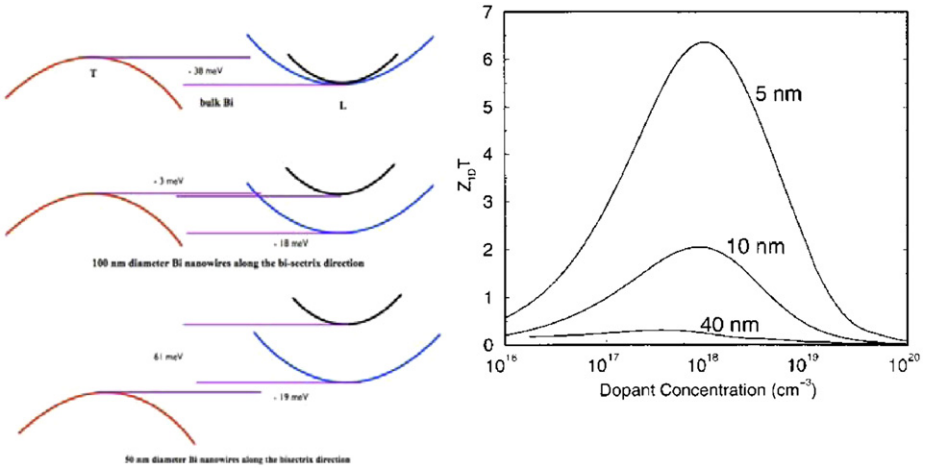

Figure 5 Schematic energy band diagram showing the energies of the sub-band edges for the heavy and light electrons and for the holes for: bulk Bi, 100 nm diameter Bi nanowires along the bisectrix direction, and 50 nm diameter Bi nanowires along the bisectrix direction. Calculated $Z_{1D}T$ for *n-type* Bi nanowires oriented along the trigonal axis at 77 K as a function of donor concentration for three different wire diameters [109].

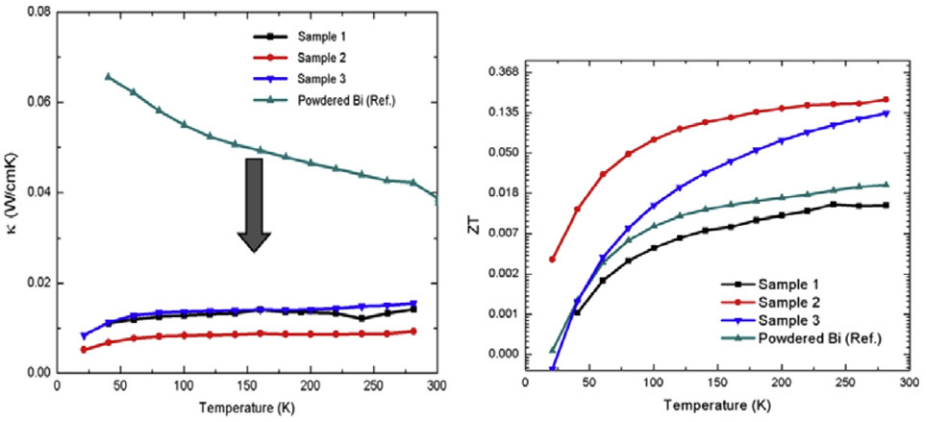

Figure 6 Thermal conductivity as a function of temperature for Bi nanostructured network samples in comparison with the Bi reference. The arrow indicates significant reduction in thermal conductivity of nanostructured Bi network samples compared to Ref. [113] Temperature dependence of figure of merit (ZT) for Bi nanostructured network samples evaluated against Bi reference [113].

Please cite this article as: H. Alam, S. Ramakrishna, A review on the enhancement of figure of merit from bulk to nano-thermoelectric materials, Nano Energy (2013), http://dx.doi.org/10.1016/j.nanoen.2012.10.005

nano-powders and then hot pressing them into dense bulk sample, 60% improvement in the ZT was achieved. The peak ZT from 0.5 to 0.8 at 700 °C was attained with nanostructured grains with the reduced thermal conductivity. Normally the grain boundaries scatter not only the phonons but also the electrons. However, in $Zr_xHf_{1-x}CoSb$ and in $Zr_xHf_{1-x}NiSn$, no decrease in carrier mobility was observed when the grain size goes from micron to nanometer. This suggests that by reducing the average grains size further down to 30–50 nm, higher ZT can be accomplished. Joshi et at studied the effect of Ti substitution for Hf in $Hf_{0.75-x}Ti^xZr_{0.25}NiSn_{0.99}Sb_{0.01}$ and found that Ti of 0.25 caused a slight increase in carrier concentration and low thermal conductivity. The ZT of about 1 at 500 K was achieved with the samples prepared with arc melting followed by ball milling and hot pressing to obtain nanostructures [118].

The nanostructures are generally obtained by ball milling the samples and 'nanostructured bulk materials' are achieved with dc current hot pressing the (ball milled) samples (Fig. 7). The major issue with the ball milling approach is the grains getting agglomerated to increased grains size.

Nanostructured skutterudites $Co_{1-x}Ni_xSb_3$ was prepared to obtain high concentration of grain boundaries to lower the thermal conductivity. The highest ZT of 0.065 has been obtained at 450 K for the conventionally prepared unfilled samples. The doping concentration and compaction have to be optimized for further enhancement [119]. Jian et al. successfully synthesized

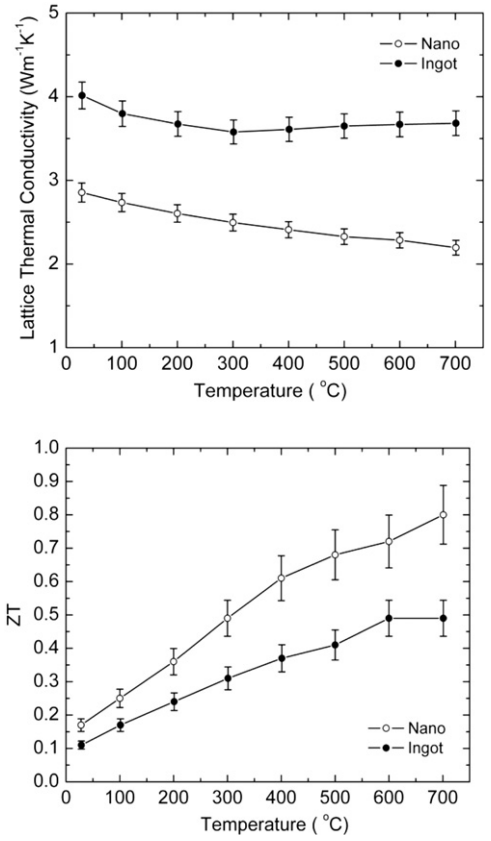

Figure 7 Temperature-dependent ZT of ball-milled and hot-pressed sample in comparison with that of the ingot [117]. Temperature-dependent lattice part of thermal conductivity of ball-milled and hot-pressed sample in comparison with that of the ingot [117].

nanostructured $CoSb_3$ in particle form of 20 nm and sheet form of 80 nm in an attempt to improve thermoelectric properties by increased phonon scattering [120]. He et al. obtained the ZT of 0.7 at 525C with $Co_{0.9}Ni_{0.09}Sb_3$ [121].

Some researchers were combined these two approaches such as enhancing the transport properties and reducing lattice thermal conductivity together. Quantum dot Superlattices (QDS) have been proposed as solution for the combination of decreased lattice thermal conductivity and quantum confinement of carriers. In QDS, the electrical conductivity is occurring due to hopping between dots. The hopping conductivity is characterized by very low mobility. Hence while using QDS, it is not worth relying on low lattice thermal conductivity but also on enhanced carrier transport. The strong coupling and regimentation was proposed to form the 3D extended mini-bands instead of localized quantum dot states. Ge quantum dots grown on Si was proposed which can be synthesized as 3D regimented QDS [122]. The strong modification in phonon group velocity results in the enhanced phonon relaxation rates because of the spatial confinements [123]. The thermal conductivity in Ge/ Si quantum dot superlattices was investigated theoretically and experimentally from the range of 10–400 K by increasing the phonon group velocity and reported the reduction of k_{ph} compared to the bulk materials [124–126].

Superlattice nanowire (SLNW) which consists of series of interlaced two different 0D QDS forming a nanowire. The electronic transport along the wire axis is made possible by the tunneling between adjacent QDs while uniqueness each QDs are maintained by the energy difference of the conduction or valance bands between different materials. Also the nanodots block the phonon conduction along the wire axis. Based on this, several materials such as Co/Cu with electrochemical deposition method and GaAs/GaP, Si/SiGe and InP/InAs with vapor liquid solid growth mechanism were synthesized. The lead salts were investigated with the theoretical model for improving the thermoelectric properties based on this concept as the lead salts such as PbTe, PbSe and PbS and their alloys are narrow-gap semiconductors that have been widely studied. The studies suggest possible enhancement of ZT of 3.3 at 77 K with PbSe of 2 nm and PbS of 8 nm [127].

Device fabrication with nanostructures

Although superlattices and nanowires give very high ZT, in order to use in large scale applications, either thin film materials or nanostructured bulk materials are adopted depending on the applications. For example, on chip integration of Peltier devices, thin films are considered more appropriate whereas for stand-alone devices, nanostructured bulk materials can be suggested.

Thin film with embedded quantum dots

Thin-film thermoelectric materials are found to offer tremendous scope for the ZT enhancement [128]. There are three generic approaches have been proposed to date. The first method uses quantum confinement effects to obtain the enhanced density of states near Fermi level [91]. With this approach, ZT of 0.9 at 300 k and 2.0 at 550 K have been achieved in $PbSe_{0.98}Te_{0.02}$/ PbTe quantum dot structures. The second approach is phonon blocking/ electron transmitting

Please cite this article as: H. Alam, S. Ramakrishna, A review on the enhancement of figure of merit from bulk to nano-thermoelectric materials, Nano Energy (2013), http://dx.doi.org/10.1016/j.nanoen.2012.10.005

superlattices. These structures utilize the acoustic mismatch between superlattices components to reduce K_{ph}. The third approach is based on thermionic effects in hetero-structures [100,109].

The nanostructured film materials made up of n type PbSeTe/PbTe QDSL were synthesized with self-assembly technique from MBE growth. The metal wire was used as a p type material to build the TE device with ZT of 1.3–1.6 at room temperature against the conservatively estimated value of 2 at 300 K[129]. In addition to lead tellurides, Bi_2Te_3 also was studied extensively and were found that none of the telluride compounds are suitable for integrated devices as these materials are not compatible with the standard IC fabrication technology [130]. Although, the polycrystalline SiGe and polycrystalline Si were found as the suitable material based on their fabrication compatibility, they are inferior to the telluride compounds as shown in Table 2. The other fabrication techniques like MOCVD and flash evaporation are still under development [130]. The telluride compounds are mostly fabricated with MEMS like technologies such as electrochemical process [131].

There was an attempt to develop thermo-ionic coolers comprising of superlattices within SiGe materials completely based on CMOS technologies as discussed above [132]. Since the thermoelectric properties of SiGe decreases at the room temperature, the devices are not suitable at certain point. Non CMOS techniques were used to develop p type B_4C and B_9C but it was limited to small place like 1 cm^2. The superlattices such as p type Bi_2Te_3/Sb_2Te_3 and the n type $Bi_2Te_3/Bi_2(Te,Sb)$ were synthesized with non CMOS technologies where cross plane transport reduced phonon thermal conductivity. The ZT was obtained as ~2.4 at 300 K [100] simulated remarkable interest in this method. In general there are two types of configurations based on transport directions i.e. in plane and cross plane superlattices with varied characteristics (Fig. 8 a and b). In the cross-plane direction, phonons are reflected while electrons are transmitted together with other mechanisms such as electron energy filtering and thermionic emission.

The thermoelectric devices based on V–IV compounds Bi_2Te_3 and $(Bi, Sb)_2Te_3$ were manufactured by thin film technology and microsystem technology [133]. The material growth c axis perpendicular to the heat flux was found to give the best device performance as it is evident from the Table 3 [134].

The membrane materials should have both thermal isolation and strength enough to support itself. Other materials such as SiO_2, SiN, SiC were found to have some attractive properties. Compared to SiO_2, the mechanical properties of low stress LPCVD SiN are more suitable. However, SiO_2 is superior when thermal properties are concerned. Besides SiO_2/ SiN, SiC/ SiN are showing good potential. It has been also observed that the thermal conductivity of polySi is so high that cooling is restricted to just below the a few kelvins than the room temperature [130]. Unlike Si/Ge superlattice, in MEMS based thermoelectric, the thermal contact resistance becomes relatively as important as the resistance of thermoelectric pairs which decreases with increasing thickness of the thin film. The vertical and horizontal architecture are made with thin film technology for power generation and cooling. Using Si/SiO_2 as a substrate, a common vertical architectures were made with thin-film sputtering deposition techniques.

Table 2 Comparison list of Bi_2Te_3, Poly SiGe and Poly Si. While Bi_2Te_3 are showing outstanding performance comparing poly SiGe and poly Si, the silicon germanium scores above Bi_2Te_3 as far as fabrication is concerned due their established IC fabrication technologies.

Materials [126,130]	Type	Seebeck coefficient (μV/K)	Resistivity (μΩ m)	Conductivity (W/mK)	ZT (10^{-3}/K)	Doping concentration (10^{20}/cm^3)
Bi_2Te_3	n type	−240	10	2.02	2.89	0.23
	p type	162	5.5	2.06	2.32	0.23
Poly SiGe	n type	−136	10.1	4.45	0.328	1–3
	p type	144	13.2	4.80	0.413	2–4
Poly Si	n type	−120	8.5	24	0.071	3.4
	p type	190	58	17	0.037	1.6

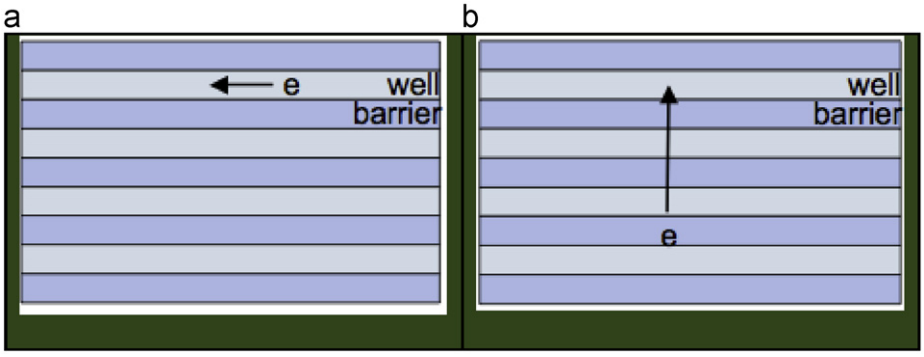

Figure 8 Quantum confinement—in plane and cross plane transport.

Please cite this article as: H. Alam, S. Ramakrishna, A review on the enhancement of figure of merit from bulk to nano-thermoelectric materials, Nano Energy (2013), http://dx.doi.org/10.1016/j.nanoen.2012.10.005

Table 3 Comparison of n Bi_2Te_3 in perpendicular *c* axis and perpendicular/parallel *c* axis ratio shows that *ZT* performance of perpendicular *c* axis is twice that of parallel *c* axis while Seebeck coefficient of the both are almost the same. The thermal conductivity is much higher in perpendicular *c* axis than its counterpart.

Property of *n* Bi_2Te_3	Perpendicular *c* axis	Perpendicular/parallel *c* axis
Seebeck coefficient (μV/K)	−115-240	−1
Specific conductivity $(\Omega\,cm)^{-1}$	600-3500	4-6
Conductivity (W/mK)	2-3	2.0-2.5
Linear thermal expansion coefficient (K)	22.2×10^{-6}	2
ZT	$1.5\text{-}3 \times 10^{-3}$	−2
Power factor (μW/cm K)	20-50	4-6

8.2 Ordered & random nanocomposites based bulk TE

Although superlattices and nanowires give very high ZT, in order to use in large scale applications, nanostructured bulk materials were proposed as an alternative to thin film materials. Since the reduced phonon thermal conductivity comes from the sequential interface scattering of phonon, using *nanocomposites* becomes potential and the cheap alternative to the expensive superlattices.

The main goal of designing materials for such applications is to introduce many interfaces for reducing the thermal conductivity more than the electrical conductivity by interfacial scattering and increasing S by carrier-energy filtering or by quantum confinement, more than decreasing the electrical conductivity. This increases power factor and there by ZT. The bulk materials act as host materials and nanomaterials become matrix materials or nanoscale materials are assembled as nanocomposites containing a coupled assembly of nano-clusters (Fig.9). The random assemblage of two kinds of nanoparticles in the heterogeneous composites or nanoparticles in host materials of the bulk can yield enhanced ZT.

Since nanocomposites materials can be handled easily from the properties-measurement/ materials-characterization point of view, they can be assembled into desired shapes and scaled up for commercial use.

However, there are challenges posed by electrons which are scattered by the randomly oriented grains and this leads to reduction of both electrical and thermal conductivities in the same material. In this case, there would be less or no change in ZT. The inclusion of BN or B_4C nanoparticles into SiGe alloy reduced both thermal and electrical conductivity contributing to nothing. Hence it is essential to reduce thermal conductivity without compromising electrical conductivity. This can be achieved by properly choosing the mismatch in the electronic properties, the electron transport properties can be maintained to the required level [135]

25% increase of ZT was demonstrated with tubular Bi_2Te_3 nanowire inclusion in Bi_2Te_3 nanocomposites since nanotubes have the structural features of holey and low dimensional materials [136]. The holey structures scatter phonons strongly while the low dimensionality influences the power factor. The nanotubes cause the reduction of the thermal conductivity without affecting the electrical conductance much while increases the figure of merit of the Bi_2Te_3 based materials. The ZT of p type bismuth antimony telluride

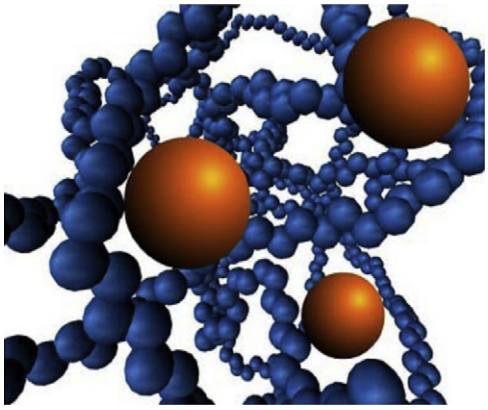

Figure 9 Nanocomposite thermoelectric material.

nanocrystalline bulk alloys were synthesized with ball milling, followed by DC hot pressing. The ZT was measured to be 1.4 at 100 °C and decreased to 0.85 at 250 °C. The ZT enhancement comes not only from phonon thermal reduction but also from the reduction of bi-polar contributions to the electronics thermal conduction at high temperature [137]. Grain growth is a major issue during the DC hot pressing the nano-powder into bulk samples. Organic agents such as oleic acid-OA solve this issue. The OA at the beginning of the ball milling reported to have suppressed the grain growth [138].

Another interesting strategy is reported by dispersing Cu nano-rods in Te as Cu_7Te_4 in $Bi_{0.4}Sb_{1.6}Te_3$ matrix. The ZT of 1.14 at 444 K was found with Cu_7Te_4-$Bi_{0.4}Sb_{1.6}Te_3$ which is 27% higher than $Bi_{0.4}Sb_{1.6}Te_3$ [139]. While Cu based collidal syntheses of monodispersed ternary and quaternary chalcogenide nanocrystals ($CuInS_2$, $CuInSe_2$ and $CuZnSnS_4$) are hot issues as inorganic solar absorbers. Fan et al. studied the impact of $Cu_2CdSnSe_4$ (CCTSe) nanoparticles of dense materials compacted from CCTSe nanoparticles-the less studied TE materials (Fig. 10). They reported the ZT of 0.65 at 450 °C [140].

Grimm et al. used micro-wave plasma induced thermal decomposition of gaseous precursors (GeH_4 and SiH_4) to synthesize semiconductor nanoparticles and mixed them with B_2H_4 and PH_3 respectively. By adjusting the fraction of the gas phase to control the dopant concentration, nano-sized SiGe materials were prepared [141]. Sheele et al. reported 60% reduction in thermal conductivity with 15-20 nm thick Sb doped $Sb_{(2-x)}Bi_xTe_3$ nanoplatelet. The ZT

Please cite this article as: H. Alam, S. Ramakrishna, A review on the enhancement of figure of merit from bulk to nano-thermoelectric materials, Nano Energy (2013), http://dx.doi.org/10.1016/j.nanoen.2012.10.005

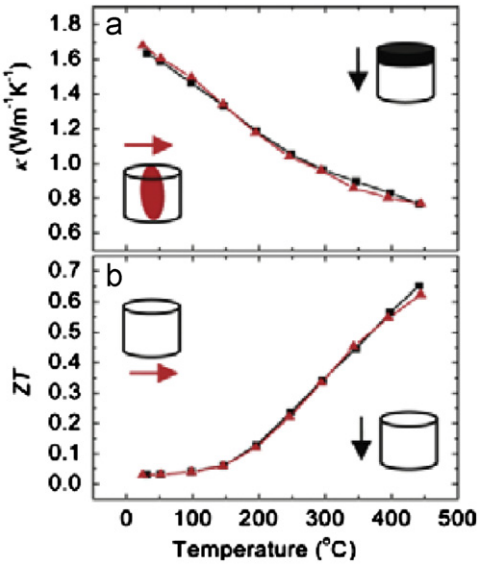

Figure 10 Temperature dependence of (a) thermal conductivity and (b) dimensionless figure-of-merit parallel and perpendicular to the pressing direction. The arrows in figures indicate the directions of the property being measured, the direction of the hot pressing is parallel to black arrows [140].

was increased by 15% compared to its bulk counterpart [142]. Yang et al. demonstrated a thermoelectric nano-generator of 1.94 nW made with non-toxic and low cost oxides Sb doped ZnO. The single Sb doped ZnO showed the Seebeck coefficient of $-350\ \mu V/K$ and a high power factor of $3.2\times10^{-4}\ W/mK^2$ [142]. ZnO has excellent charge carrier transport which are tunable via doping [143]. Zhou et al. grew Ga doped ZnO nanowires array which were well aligned and uniform, with a simple chemical vapor deposition method [144]. These processes made ordered nanocomposites possible to obtain many advantages over random nanocomposites.

About 50% improvement of ZT from 0.65 to 0.95 at 800-900 K was reported with an atomic ratio of $Si_{80}Ge_{20}$ doped with boron. The reason for the high ZT was attributed with the reduction of thermal conductivity due to the increased phonon scattering form the high density nano-grain interfaces in the nanocomposite. The theoretical study with Si nanocomposite with 10 nm was also found to have ZT above 1 at 1000 K. Comparing SiGe alloy Si nanocomposite is more advantageous than expensive germanium [145].

Soni et al. demonstrated that Se doped $Bi_2Te_{3-x}Se_x$ nanoplatelet composites enhanced ZT by nearly a factor of 4 to $ZT=0.54$ at 300 K where $x=0.3$ in comparison with Bi_2Te_3 nanocomposites (Fig. 11). This group achieved it by synthesizing by polyol method [146]. The enhancement is attributed to the energy filtering of low energy electrons by ordered nanocomposites with plenty of grains.

Fabrication of nanocomposites

Apart from growing nanoscale materials by epitaxial methods, cheaper bulk materials with a nanoscale structures are more attractive. One is based on mechanical alloying and sintering of the mixtures [147] and the next is based on rapid cooling of homogeneous multi component melts exhibiting large miscibility gaps in solid state in the respective phase diagram [148]. The nanocomposites are produced by first synthesizing thermoelectric nanoparticles and then assembling into dense bulk solids. The thermoelectric nanoparticles are prepared by wet chemical reaction, the hydrothermal method and high energy ball milling [149]. The high energy ball milling is an effective top-down approach to make thermoelectric nanomaterials. The nanocomposites are assembled into bulk solid by the spark plasma sintering, cold pressing, sintering and extrusion methods [150]. The combination of high energy ball milling and hot pressing is attractive combination from commercial point of view due to its mass scale production.

The nanostructured p type SiGe bulk alloys were prepared by the low cost ball milling and DC induced hot press compaction process [151], not by the expensive and slow atomic layer deposition process [114]. The Bi_2Te_3, SiGe alloys and skutterudite $CoSb_3$can be produced with high energy ball milling and hot pressing method [152]. The materials of V-VI and IV-VI groups such as Bi_2Te_3 and PbTe are fabricated by sintering with spark plasma sintering—a relevant technique for compaction of nanostructured powders. Yucheng et al. gives a summarized table of thermoelectric materials prepared by hot pressing and ball milling method in Ref. [152]. The chemical synthesis and spark plasma sintering method are also employed to produce thermoelectric nanoparticles and nanocomposite respectively [153]. Alexis et al. fabricated a device comprised of Si nanowires embedded in a polymer matrix. They used vapor–liquid–solid (VLS) growth mechanism because single-crystalline nanowires comprised of a wide range of materials can be synthesized with control of doping, diameter and growth orientation [154]. Zhu et al. prepared Na_xCoO_2/Co_3O_4 layered nanocomposite through exfoliation, stacking and sintering processes and observed the electrical conductivity to be 120 S/cm at 1200 K which is comparable with $Na_{0.7}CoO_2$ [155].

Despite of several recent reports on wet chemical synthesis preparation of thermoelectric nanoparticles such as bismuth tellurides, CZTSe and its analogs, only a few reports show a significant progress in thermoelectric properties. Compacting or annealing procedures from several batch processes due the low scale production, in the range of ten to hundreds of milligrams, cause the variations in the chemical composition and particle sizes in the nanocomposite bulk TE materials [140]. Feng-Jia Fan very recently demonstrated large scale colloidal synthesis of CSTSe nanocrystals which have attracted intensive attention due its good thermoelectric properties after being doped. They achieved the output of 10 g of $Cu_2ZnSnSe_4$ in a single batch. The dense materials were obtained by hot-pressing at different temperatures and obtained ZT of 0.44 at 450C which is comparable to the state of the art ZT values of CZTSe or CTSe based materials at the similar temperature (Fig. 12) [156]. They further report that this synthesis procedure is highly extendable, in principle, therefore other binary, tertiary and quaternary selenide nanocrystals could be possible through this method.

Model calculations provide an important guide for the design and choice of processing parameters in the preparation of the nanocomposite structures. In an aligned-nanoparticles with periodic boundary conditions and temperature difference, solution of the Boltzmann transport eq. is used whereas for

Please cite this article as: H. Alam, S. Ramakrishna, A review on the enhancement of figure of merit from bulk to nano-thermoelectric materials, Nano Energy (2013), http://dx.doi.org/10.1016/j.nanoen.2012.10.005

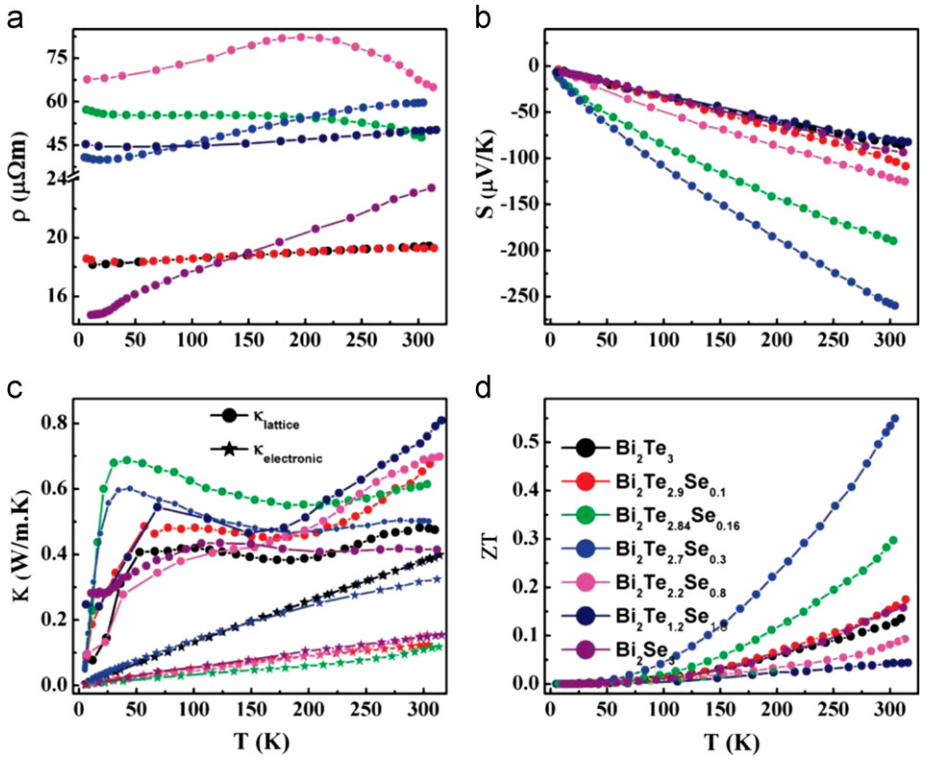

Figure 11 Temperature dependence of the (a) electrical resistivity, (b) thermoelectric power, (c) lattice (κl) and electronic (κe) thermal conductivities (estimated from the Wiedemann-Franz law; see text for details) and (d) thermoelectric figure of merit of Bi2Te3−xSex NP composites. All the figures share the same color notations as shown in (d) [146].

random unit cells, Monte Carlo methods are more suitable. Though Boltzmann transport equation and Monte Carlo methods have been used for modeling the nanocomposites, there are still challenges in optimizing their process conditions and doping species. The wavelength (λ) and mean free path (MFP) for phonons (or electrons) at certain energy are unknown for most materials system and this makes the theoretical predication of thermal conductivity (electronic conductivity) extremely difficult for nanocomposite with varying-size inclusions [157].

Future road map of nanocomposites

Si being abundant and widely used semiconductor, nanocomposites in thin film is expected to grow and contribute to improve the thermal management in microelectronics industries. The main advantage of using Si nanowires for thermoelectric applications lies in the large difference in mean free path lengths between electrons and phonons at room temperature [158]. By using roughened silicon nanowires, the thermal conductivity was reduced to~1.6 W/mK, with the phonon contribution close to the amorphous limit, with no much compromise on power factor so that ZT was achieved to near unit at the room temperature. Instead of random nanocomposite, ordered nanocomposites have proven better and hence have good potential. It is not still understood clearly which carriers are dominant heat/ charge carrier, what the optimal size distribution is and the type of interfaces that lead strong phonon scattering and the weak electrons [157].

The energy filtering techniques are used to filter phonons and allow high energy electrons to pass through. This increases the Seebeck coefficient due to the negative Seebeck distribution. However, it will not be simple to filter energy by mere controlling the grain boundaries as it is related to the electron mobility. The mobility of electrons through the grain in n type $Si_{80}Ge_{20}$ for example, decreases by 40% in the experimental results comparing the theoretical calculations. The density of states can be increased by introducing energy level created by impurities. Due to these impurities, the energy levels lie in the conduction or valence bands creating the resonant level and a local maximum in the electronic density of states. It was experimentally tested with PbTe by introducing Tl in it. Another challenge is to reduce electronic thermal conductivity completely without disturbing its conductivity and predicted that materials with such characteristics are not likely in near future [159]. Apart from improving the intrinsic energy conversion efficiency of the materials, there are attempts from the perspective of systems architectures. There are three general approaches proposed. The first approach is to look for design optimization and reduce parasitic losses by using non-traditional materials in device fabrication. The second approach is to determine if alternative thermodynamic cycle could be used to improve efficiency. The third proposed approach comes from the realization that there is no length scale in the equations that determines the efficiency of a thermoelectric engine [160].

Gaining the greater insights of electron and phonon scattering at the grain boundary and adopting the suitable fabrication techniques to produce it will determine the future course of action. This will give the opportunities of adopting the ordered nanocomposites instead of random nanocomposite for high ZT thermoelectric materials [117].

Please cite this article as: H. Alam, S. Ramakrishna, A review on the enhancement of figure of merit from bulk to nano-thermoelectric materials, Nano Energy (2013), http://dx.doi.org/10.1016/j.nanoen.2012.10.005

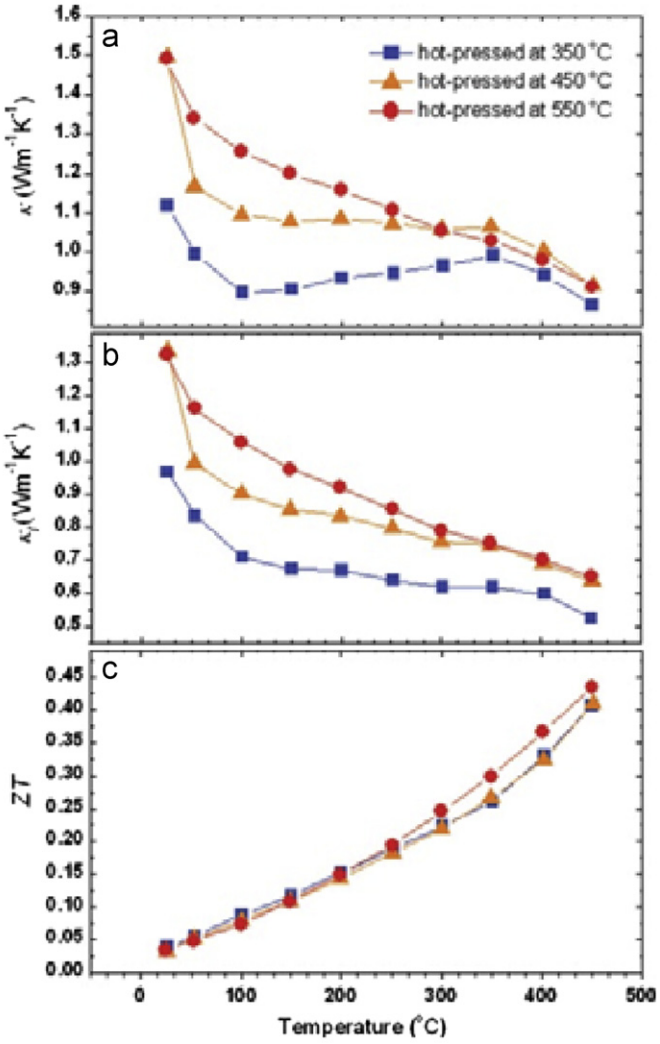

Figure 12 Temperature dependence of: (a) thermal conductivity (κ), (b) lattice thermal conductivities and (c) *ZT* [156].

Future potential applications

There are significant commercial values in developing next generation integrated cooling systems and power generation from the waste energies. Many of the existing micro-sensors and micro-actuators can be modified based on the thermoelectric principle. They use thin-film approach to achieve sensing and actuator functionality, fabricated with micromachining techniques to achieve device optimization. However, the development of thermoelectric devices compatible with standard semiconductor process has huge potential to address many applications in microelectronics, made with MEMS technology, along with nanotechnology [117].

Micro-thermoelectric devices fabricated with thin-film technology, have achieved sufficient miniaturization that can be integrated with microelectronics or semiconductor devices instead of mounting them externally. As semiconductor industry further reduces the size of transistors in ICs, a trend is to fabricate more of the external circuitry inside the semiconductor packaging. The next generation ICs will thus be possible if the thermal management is appropriately executed since the performance is directly proportional to power. If the failure rate is targeted to 1000–5000 FITs (failures in Terra hours), the successful thermal packaging should rely on a judicious combination of materials and heat transfer mechanisms those stabilize the component temperature at an acceptable level.

Since the electronics and opto-electronics need only a small scale or a localized spot cooling of very tiny components, thermoelectric solutions are more appropriate than bulk inefficient conventional cooling systems such as fans and fins. However, if a significant economical cooling can be achieved, the computing speed of some CMOS computer processors gains about 30–200% [36]. There are two startup companies working on thin film based thermoelectric devices. One company uses MEMS like sputtering deposition and Bi_2Te_3 related materials while other uses Bi_2Te_3-Sb_2Te_3 superlattice technology. The later approach seems to be compatible with modern semiconductor processing techniques.

Nanoscale or nanocomposites based thin film thermoelectric materials find potential applications in several industries including microelectronics, infrared detector, CCD, LED, optoelectronics cooling. Energy harvesting or scavenging systems is expected to replace the conventional batteries one day. For the waste heat recovery from the vehicle exhaust (at 350 °C temperature differential), the efficiency needs to be about

Please cite this article as: H. Alam, S. Ramakrishna, A review on the enhancement of figure of merit from bulk to nano-thermoelectric materials, Nano Energy (2013), http://dx.doi.org/10.1016/j.nanoen.2012.10.005

10% and the corresponding ZT is 1.25 to increase the mileage up to 10%. For the primary power generation, the net efficiency needs to be about 20% and have an average ZT of 1.5 or higher at 800C temperature difference.

The sensors based on nano-thermoelectric materials find huge applications in life sciences as well. The applications those requiring temperature change function such as fast DNA analysis on a nanoliter scale, continuous environmental or hazard assaying, real-time monitoring of complex biological processing, and to control the power supplies for remote-sensing systems, are potential ones. Gains of about 5–10% would be possible in diesel powered co-generators that are becoming widely used for onsite power generation in developed countries and for 5000–20,000 W primary generators in developing countries. In another proposed co-generator concept, the solar spectrum is split into shorter wavelengths that yield high photovoltaic-conversion efficiency and longer wavelengths that heat thermoelectric generators.

At ZT is 2, it appears to replace small internal combustion engines such as those used in lawn movers, blowers, and outboard motorboats. These engines would be very quiet and nearly vibration free. They could burn a wide spectrum of fuels like propane, butane, LNG and alcohols and would not necessarily depend on fossil oil as a fuel source. In power generation, the cold side of the thermocouple is to be ventilated more efficiently in order to maintain the appropriate temperature differences, in many situations. Similarly the effective cooling applications need the hot end to be maintained properly. The carbon nanotube micro-fin architecture with the thermoelectric systems proves to be more effective. The tiny cooling elements made up of multi walled carbon nanotubes mounted on the systems enable the efficient power dissipation [1].

Conclusions

The thermal management is a major problem everywhere and every day. On the other hand there are heavy demands for energy.Thermoelectric concept seems to be one of most suitable solutions for these problems. However, there are challenges in choosing suitable materials with sufficiently higher ZT for the applications. The best thermoelectric materials were succinctly defined as "phonon-glass electron-crystal", which means that the materials should have a low lattice thermal conductivity as in a glass, and a high electrical conductivity as in a crystal.

The interrelationships among the transport properties have been posing difficult challenges to the research community for almost four decades in achieving ZT. The attempts to increase ZT in bulk materials were not so much successful and ZT was just approaching 1.2 in TAGS materials. The ZT of SiGe bulk materials are less than 1 at 900 K. However, Bi_2Te_3 and PbTe are widely used bulk materials in high temperature applications. The ZT of Bi_2Te_3 crystalline materials are about 0.75 and 0.86 at room temperature.

The complex structures helped enhance ZT with various approaches mainly by clathrates, skutterudites and zintl phase. The substructure approach and incorporating nanostructures opened up new doors. Researchers could achieve ZT up to 2.5 at room temperature in superlattices. However the fabrication of superlattices is expensive and not suitable for scaling up for mass production.

The recent understanding of phonon scattering and the energy filtering led the development of nanocomposites which scatters the phonon randomly. The nanocomposites are showing promising route to develop materials of higher ZT. However, the mechanism has not been understood well. By properly choosing the mismatch in the electronic properties, the electron transport properties can be maintained to the required level in nanocomposites. The fabrication cost of producing nanocomposite, unlike the superlattices, is expected to be affordable. There are continuous efforts to increase the figure of merits of the bulk materials with the inclusion of nanocomposites.

Apart from approaching the problem of enhancing the efficiency from the intrinsic properties, the system approaches can also be made. By proper architectural design, the efficiency of thermoelectric system can be increased. The integration of various other materials like carbon nanotubes for power dissipation properties and novel graphene properties for high electric conductivity at the junctions can also be incorporated going forward in future.

Since the laws of thermodynamics do not set any upper limit on ZT, still there are scopes to increase the efficiency and potential applications can be found apart from some discussed earlier. As the ZT is increasing higher and higher, it keeps opening up more and more of potential applications in

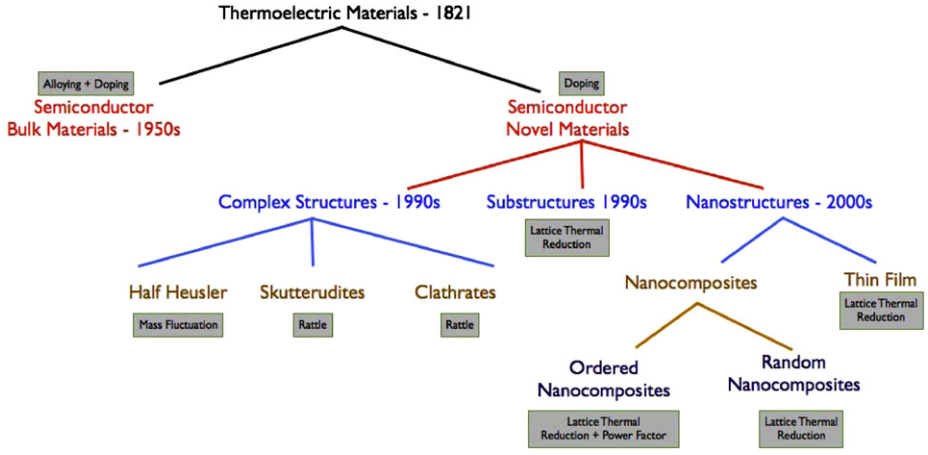

Figure 13 History of Efforts in increasing ZT.

Please cite this article as: H. Alam, S. Ramakrishna, A review on the enhancement of figure of merit from bulk to nano-thermoelectric materials, Nano Energy (2013), http://dx.doi.org/10.1016/j.nanoen.2012.10.005

daily life, life science, military, space and energy sectors. The below image Fig. 13 shows the direction of development of thermoelectric materials since 1950s.

References

[1] K. Kordas, G. Toth, P. Moilanen, M. Kumpumaki, J. Vahakangas, A. Uusimaki, R. Vajtai, P.M. Ajayan, Applied Physics Letters 90 (2007) 123105.

[2] A. Bar-Cohen, A.D. Kraus, S.F. Davidson, Design and Packaging of Microelectronic Equipment Engineering 105 (6) (1983) 5359.

[3] L.T. Yeh, Journal of Electronic Packaging 117 (1996) 333–339.

[4] Kaveh Aza-Chip Level Spot Cooling, Chip Scale Review, pp 17–19, May/ June 2011.

[5] Laser Cooling for TO Packages using Embedded Thin-Film Thermoelectric Coolers-Nextreme Thermal Solutions, Inc., 〈http://www.nextreme.com/media/pdf/Nextreme_Laser_Diode_Cooling_Test_Report_Jan10.pdf〉, January 2010 (accessed 10 07.12).

[6] 〈http://www.mcleancoolingtech.com〉 (accessed 13.07.12).

[7] 〈http://www.koolatron.com〉 (accessed 19.07.12).

[8] Isabelle Caplain, Fabrice Cazier, Habiba Nouali, Agnès Mercier, Jean-Claude Déchaux, Valérie Nollet, Robert Joumard, Jean-Marc André, Robert Vidon, Atmospheric Environment 40 (31) (2006) 5954–5966.

[9] Raghavendra Nunna, Emmanuel Guilmeau, Franck Gascoin, Synthesis and characterization of novel intermetallics for thermoelectric conversion, Journees de l'Ecole Doctorale Simem (UCCBN) les 24 et 25 avril (2012).

[10] Tawee Pogfai, Krongkamol Wong-ek, Suriya Mongpraneet, Anurat Wisitsoraat, Adisorn Tuantranont, International Journal of Appled Biomedical Engineering 1 (1) (2008).

[11] D.M. Rowe, International Journal of Innovations in Energy Systems and Power 1 (1) (2006).

[12] G. Jeffrey Snyder, The Electrochemical Society Interface (2008) 54–56.

[13] 〈http://www.gmzenergy.com/〉 (accessed 1.08.12).

[14] Giulio Casati, Carlos Mejia Monasterio, Tomaz Prosen, Physical Review Letters 101 (2008) 016601.

[15] D.M. RoweEd. Introduction, CRC Handbook of Thermoelectrics, 1995.

[16] Herwin Ahuja, Bao Yang, Thanh N. Tran, HVAC&R Research 14 (5) (2008) 635–653.

[17] Giuliano Benenti, Giulio Casati, Philosophical Transactions of the Royal Society A (2012) 466–481.

[18] Ing. Julio Cesar Contreras Vargas, Jorge Luis Díaz Rodríguez, Aldo Pardo GarcíaMauricio Figueroa, A Peltier Cells Research - (First Part)—Revista Colombiana de Tecnologías de Avanzada, Volumen 1—Número 11—Enero 2008.

[19] H.J. Goldsmid, in: D.M. Rowe (Ed.), CRC Handbook of Thermoelectrics, CRC Press, 1995.

[20] S.B. Riffat, Guoquan Qiu, Applied Thermal Engineering 24 (14–15) (2004) 1979–1993.

[21] Jiao Wang, Guilio Casati, Tomaz Prosen, C.H. Lai, Physical Review E 80 (2009).

[22] G.A. Slack, in: H. Ehrenreich, F. Seitz, D. turnbull (Eds.), Solid State physics, 34, Academic Press, 1979.

[23] P. Pichanusakorn, P. Bandaru, Materials Science and Engineering R 67 (19) (2010) 19–63.

[24] M. cutler, J.F. Leavy, R.L. Fitzpatrick, Physics Review 133 (1964) A1143–A1152.

[25] G.Jeffrey Snyder, S Toberner Eric, Nature Materials 7 (2008) 105–114.

[26] H.J. Goldsmid, Introduction to Thermoelectricity, Springer, Berlin Heidelberg, 2010. ISBN: 978-3- 642-00716-3.

[27] Weishu Liu, Xiao Yan, Gang Chen, Zhifeng Ren, Nano Energy 1 (2012) 42–56.

[28] Alexander A Balandin, Evghenii P Pokatilov, D.L. Nika, Journal of Nanoelectronics and Optoelectronics 2 (2007) 140–170.

[29] G.D. Mahan, J.O. Sofo, Applied Physical Sciences 93 (1996) 7436–7439.

[30] T.M. Tritt, Annual Review of Materials Research, in: Encyclopedia of Materials: Science and Technology, Elsevier, 2002. ISBN: 0-08- 043152-6.

[31] Ali Shakouri and Suquan Li, Proceedings of International Conference on Thermoelectrics, Baltimore, September 1999.

[32] J.A. Ewing, Effects of Stress on the Thermoelectric Quality of Metals. Part I Proceedings of the Royal Society of London, pp 399–402, 1881.

[33] Shelford Bidwell, On the Changes of Thermoelectric power Produced by Magnetization and their relation to Magnetic Strains, Proceedings of the Royal Society of London, pp 413–434, 1904.

[34] L.C.F. Blackman, P.H. Dundas, A.R. Ubbelohde, The Anisotrpic Thermoelectric Power f Graphite, Proceedings of the Royal Society of London A, 255 pp 293–306, 1960.

[35] A.R. Allnat and P.W.M. Jacobs, Thermoelectric Power of Ionic Crystals. II. Results of Potassium Chloride, Proceedings of the Royal Society of London A, 260, pp 350–369, 1961.

[36] A.R. Allnat and P.W.M. Jacobs Thermoelectric Power of Ionic Crystals. II. Results of Potassium Chloride, Proceedings of the Royal Society of London A, 267, pp 31–44, 1962.

[37] Giuliano Keiji Saito, Giulio Casati Benenti, A microscopic mechanism for increasing thermoelectric efficiency, Chemical Physics 375 (2010) 508–513.

[38] A.F. Ioffe – Thermoelements, Thermoelectric Cooling, Infosearch Limited, London, 1957.

[39] Duck Young chung, Tim Hogan, Paul Brazis, Melissa Rocci Lane, Carl Kannewurf, Martina Bestea, Ctirad Uher, Mercourni G Kanatzidis, Science 287 (2000) 11 February.

[40] E.A. Skrabek, D.S. Trimmer, in: D.M. Rowe (Ed.), CRC Handbook of Thermoelectrics, CRC Press, 1995.

[41] Yoichi Ando, N. Miyamoto, Kouji Segawa, T. Kawata and I. Teasaki, Specific heat evidence for strong electron correlations in the thermoelectric materials (Na, Ca)Co2O4, arXiv, 1999.

[42] I. Terasaki Transport Properties and Electronic state of the Thermoelectric Oxide NaCo2O4—arXiv: cond - mat/0207315v1, 12 July 2002.

[43] Tadashi Mochida Kenjiro Fujita, - Kazuo Nakamura, Japanese Journal of Applied Physics 40 (2001) 4644–4647.

[44] Ohtaki, Y. Nojiri and E. Maeda, Proceedings of the Nineteenth International Conference on Thermoelectrics (ICT2000), Babrow, Wales, p. 190, 2000.

[45] J. Sugiyama, J.H. Brewer E.J. Ansaldo, H. Itahara, T. Tani, M. Mikami, Y. Mori, T. Sasaki, S. Hebert and A. Maignan – Dome, Shaped Magnetic Phase Diagram of Thermoelectric Layered Cobaltites—arXiv: cond - mat/0310516v1, 2003.

[46] Hiromichi Singo Ohta, Masahiro Hiranto, Hedeo Hosono, Applied Physics Letters 87 (2000).

[47] G. Jeffry Snyder, M. Christensen, E. Nishibori, T. Caillat, B.B. Iversen, Nature Materials 3 (2004).

[48] T. Caillat, J.-P. Fleurial, A. Borshchevsky, Journal of Physics and Chemistry of Solids 58 (1997) 1119–1125.

[49] Weishu Bo Yua, Shuo Liua, Hui Chena, Hengzhi Wanga, Gang Wanga, Nano Energy 1 (3) (2012) 472–478.

[50] Mildred S. Dresselhaus, Gang Chen, Ming Y Tang, Gonggui Yang, Hohyun Lee, Dezhi Wang, Zhifeng Ren, Jean-Pierre Fleurial, Pwan Gonga, New Directions for Low Dimensional Thermoelectric Materials-Advanced Materials (2007) 1043–1053.

[51] C. Wood, Reports of Progress in Physics 51 (1988) 459.

[52] S. Bhattacharya, A.L. Pope, R.T. Littleton IV, T.M. Tritt, Applied Physics Letters 77 (16) (2000).

Please cite this article as: H. Alam, S. Ramakrishna, A review on the enhancement of figure of merit from bulk to nano-thermoelectric materials, Nano Energy (2013), http://dx.doi.org/10.1016/j.nanoen.2012.10.005

[53] Q. Shen, L. Chen, T. Goto and T. Hirai, J. Yang, G.P. Meisner and C. Uher, Applied Physics Letters, 79, 25 4165–4167.
[54] V.M. Browning, S.J. Poon, T.M. Tritt, A.L. Pope, S. Bhattacharya, P. Volkov, J.G. Song, V. Ponnambalam, A.C. EhilichThermoelectric Properties of the Half Heusler Compound (Zr, Hf)(Ni, Pd)Sn, MRS Symposium Proceedings: Fall, In: T.M. Tritt, M. Kanatzidis, H.B. Lyon Jr, G.D. Mahan (Material Research Society, Warrendale, PA) pp 403–412, 1999.
[55] Hiroaki Muta, Takanori Kanemitsu, Ken Kuroasaki, Shinsuke Yamanaka, Material Transations 47 (6) (2006) 1453–1457.
[56] Pengfei Qiu, Jiong Yang, Xiangyang Huang, Xihong Chen, Lidong Chen, Applied Physics Letter 96 (2010).
[57] Takeyuki Sekimoto, Ken Kurosaki, Hiroaki Muta, Shisuke Yamanaka, Material Transations 46 (7) (2005) 1481–1485.
[58] Wan Ting Wu, Xiaoya Jiang, Yanfei Li, Journal of Applied Physics 102 (2007).
[59] Ting Wu, Wan Jiang, Xiaoya Li, Shengqiang Bai, Shengcong Liufu, Lidong Chen, Journal of Alloys and Compounds 467 (2009) 590–594.
[60] Pengfei Qiu, Xiangyang Huang, Xihong Chen, Lidong Chen, Journal of Applied Physics 106 (2009).
[61] Takeyuki Sekimoto, Ken Kurosaki, Hiroaki Muta, Shisuke Yamanaka, Material Transations 48 (8) (2007) 2079–2082.
[62] L.L. Wang, L. Miao, Z.Y. Wang, W. Wei, R. Xiong, H.J. Liu, J. Shi, X.F. Tang, Journal of Applied Physics 105 (2009) 013709.
[63] G.A. Slack - New, in: D.M. Rowe (Ed.), CRC Handbook of Thermoelectrics, 1995.
[64] G.S. Nolas, J. Poon, M. Kanatzidis, Materials Research Society Bulletin 31 (2006) 199–205.
[65] K. Kurosaki, A. Kosuga, H. Muta, M. Uno, S. Yamanaka, Applied Physics Letters 87 (2005) 061919.
[66] Sung Jin Kim, Siqing Hu, Ctirad Uher, Tim Hogan, Baoquan Huang, John D Corbett, Mercouri G Kantatzidis, Journal of Solid State Chemistry 153 (2000) 321–329.
[67] Norihito L Okamoto, Min Wook Oh, Takumi Nishii, Katsushi Tanaka, Haruyuki Inui, Journal of Applied Physics 99 (2006).
[68] G.S. Nolas, J.L. Cohn, G.A. Slack, S.B. Schjuman, Applied Physics Letter 73 (1998) 178.
[69] Bo B. Iversen, Anders E.C. Palmqvist, David E. Cox, George S. Nolas, Galen D. Stucky, Nick P. Blake, Metiu Horia, Journal of Solid State Chemistry 149 (2000) 455–458.
[70] G.S. Nelos, J.L. Cohn, G.A. Slack, S.B. Schujman, Applied Physics Letters 73 (2) (July 1998) 178–180.
[71] Rüdiger F.W. Herrmann, Katsumi Tanigaki, Tetsuji Kawaguchi, Sadanori Kuroshima, Otto Zhou, Physical Review B 60 (1999) 13245.
[72] Norihito L. Okamoto, Kyosuke Kishida, Katsushi Tanaka, Haruyuki Inui, Journal of Applied Physics 100 (2006).
[73] A. Bentien, M. Christensen, J.D. Bryyan, A. Sanchez, S. Paschen, F. Steglich, G.D. Stucky, B.B. Iversent, Physical Review B 69 (2004).
[74] Xiaowei Hou, Yanfei Zhou, Li Wang, Wenbin Zhang, Wenqing Zhang, Lidong Chen, Journal of Alloys and Compounds 482 (2009).
[75] D. Cederkrantz, A. Saramat, G.J. Snyder, A.E.C. Palmqvist, Journal of Applied Physics 106 (2009).
[76] Li Wang, Li Dong Chen, Xi Hong Chen, Wen Bin Zhang, Applied Physics 42 (2009).
[77] Masahiro Hokazono, Hiroaki Anno, Kakuei Matsubara, Materials Transactions 46 (7) (2005) 1485–1489.
[78] Takeshi Eto, Kengo Kishimoto, Kenji Koga, Koji Akai, Tsuyoshi Koyanagi, Hiroaki Anno, Terumitsu Tanaka, Hiroki Kurisu, Setsuo Yamamoto, Mitsuru Matsuura, Materials Transactions 50 (3) (2009) 631–639.
[79] Koji Akai, Kenji Koga, Mitsuru Matsuura, Materials Transactions 48 (4) (2007) 684–688.
[80] M. Falmbigl, G. Rogl, P. Rogl, M. Kriegisch, H. Muller, E. Bauer, M. Reinecker, W. Schranz, Journal of Applied Physics 108 (2010).
[81] Shukang Deng, Yuta Saiga, Koichiro Suekuni, Toshiro Takabatake, Journal of Applied Physics 108 (2010).
[82] Shukang Deng, Yuta Saiga, Kousuke Kajisa, Toshiro Takabatake, Journal of Applied Physics 108 (2010).
[83] Ya. Mudryka, P. Rogla, C. Paulb, S. Bergerb, E. Bauerb, G. Hilscherb, C. Godartc, D.H. Noe.le, A. Sacconef, R. Ferrof, Physica B 328 (2003) 44–48.
[84] G.S. Nolas, J.L. Cohn, J.S. Dyck, C. Uher, Physical Review B 65 (2002).
[85] F. Chen, K.L. Stokes, G.S. Nolas, Journal of Physics and Chemistry of Solids 63 (2002) 827–832.
[86] Julia V. Zaikina, Walter Schnelle, Kirill A. Kovnir, Andrei V. Olenev, Yuri Grin, V Shevelkov Andrei, Solid State Science 9 (2007) 664–671.
[87] bobeb Svilen, C Sevov Slavi, Journal of American Society 123 (2001) 3389–3390.
[88] G.S. Nolas, D.G. Vanderveer, A.P. Wilkinson, J.L. Cohn, Journal of Applied Physics 91 (11) 1 91 (11) (2002).
[89] X. Shi, W. Zhang, L.D. Chen, J. Yang, Physical Review Letter 95 (18) (2005).
[90] Bryan C Chakoumakos, Brian C Sales, David Mandrus, Eerle Keppens, Acta Crystallographia Section B (1999).
[91] Hiroyuki Tanahashi, Yoriko Ohta, Hiroshi Uchida, Yoshuio Itsumi, Akio Kasama, Kakuei Matsubara, Materials Transaction 43 (5) (2002) 1214–1219.
[92] Geoff D. Staneff, Paul D. Asimow, Thierry Caillat-Synthesis and Thermoelectric Properties of Ce(Ru0.67Rh0.33)4Sb12. Materials Research Society Symposium Proceedings, Materials Research Society, vol. 793, 2004.
[93] X. Shi, H. Kong, C.P. Li, C. Uher, J. Yang, J.R. Salvador, H. Wong, L. Chen, W. Zhang, Applied Physics Letter 92 (2008) 182101.
[94] G.S. Nolas, D.T. Morelli, Terry M Tritt, Annual Reviews Materials Science (1999) 89–116.
[95] S.Q. Bai, X. Shi, L.D. Chen, Applied Physics Letters 96 (2010).
[96] Jae - Yong Jung, Son Chul Ur, Il Ho Kim, Journal of Ceramic Processing Research 10 (2) (2009) 158–161.
[97] Jae - Yong Jung, Kwan Ho Park, Soon Mok Choi, Il Ho Kim, Won Seon Seo, Journal of Korean Physical Society 57 (4) (2010) 773–777.
[98] Jiong Xun Shi, James R Yang, Miaofang Salvador, Jung Y Chi, Hsin Cho, Shengqiang Wang, JihuiYang Bai, zhang Wenqing, Chen Lidong, Journal of the American Chemical Society 133 (2011) 9.
[99] Yu Yang Wang, Fang Sui, Luxiang Li, Xianjie Xu, WenhuiSu Wang, Liu Xiaoyang, Nano Energy 1 (3) (2012) 456–465.
[100] Sandra Franck Gascoin, Daniel Ottensmann, Sossina M Stark, Haile, G.J. Snyder, Advanced Functional Materials 0000,00 (2005) 1–6.
[101] Edward Rama Venkatasubramanian, Thomas Siivola, Colpitts, Brooks O Quinn, Nature 413 (11) (2001) 597–602.
[102] R. Fletcher, M. Tsaousidou, P.T. Coleridge, Y. Feng, Z.R. Wasilewski, Physica E 12 (2002) 478–481.
[103] Alexander Balandin, Kang L Wang, Journal of Applied Physics 84 (11) (1998) 6149–6153.
[104] L.D. Hicks, T.C. Harman, X. Sun, M.S. Dresselhaus, Physical Review B 53 (16) (1996).
[105] M.S. Dresselhaus, G. Dresselhaus, X. Sun, Z. Zhang, S.B. Cronin, T. Koga, Low Dimensional Thermoelectric Materials, Физика твердого тела, том 41, вып. 5, 1999.
[106] P Heremans Joseph, Vladimir Jovovic, Eric Toberer, Ali Saramet, Ken Kurosaki, Anek Charoenphakdee, Shinsuke Yamanaka, G. Jeffrey Snyder, Science 321 (2008) 554–557.

Please cite this article as: H. Alam, S. Ramakrishna, A review on the enhancement of figure of merit from bulk to nano-thermoelectric materials, Nano Energy (2013), http://dx.doi.org/10.1016/j.nanoen.2012.10.005

[107] T. Koga, X. Sun, S.B. Cronin, M.S. Dresselhaus, Applied Physics Letters 73 (20) (1998) 2950–2952.
[108] Herald Bottner, Gang Chen, Rama Venkatasubramanian, MRS Bulletin 31 (2006).
[109] Yu Ming Lin, Xiang zhong Sun, M.S. Dresselhaus, Physical Review B 62 (7) (2000).
[110] Ke Akram Boukali, Xu, James R Heath, Advanced Materials 18 (2006) 864–869.
[111] Balandin Alexander, Phys. Low Dim. Structure 5/6 (2000) 73–91.
[112] Jianhua Zhou, Jea Chuangui Jin, Hun Seol Xiaoguang Li, Li Shi, Applied Physics Letters 87 (2005).
[113] Gayatri Keskara, Eswaramoorthi Iyyamperumala, Dale A. Hitchcockb, Jian Heb, M. Apparao, C. Raob, Lisa D. Pfefferle, Nano Energy Available online 28 (July 2012).
[114] S.M. Lee, D.G. Cahill, R. Venkatasubramanian, Applied Physics Letters 70 (1997) 2957.
[115] R. Venkatasubramanian, Physics Review. B 61 (2000) 3091–3097.
[116] Joshua Woochul Kim, Arthur Zide, Dmirtri Gossard, Susane Klenov, Ali Stemmer, Shakouri, Arun Majumdar, Physical Review Letters PRL (2006) 96.
[117] Xiao Yan, Giri Joshi, Weishu Liu, Yucheng Lan, Hui Wang, Sanyeop Lee, J.W. Simonson, S.J. Poon, T.M. Tritt, Gang Chen, Z.F. Ren, Nano Letters 11 (2011) 556–560.
[118] Giri Joshi, Tulashi Dahal, Shuo Chen, Hengzhi Wang, Junichiro Shiomi, Gang Chen , Zhifeng Ren, Enhancement of thermoelectric figure-of-merit at low temperatures by titanium substitution for hafnium in n-type half-Heuslers $Hf_{0.75-x}TixZr_{0.25}NiSn_{0.99}Sb_{0.01}$ Nano Energy (online; but in press).
[119] Luca Bertini, Christian Stiewe, Muhammet Toprak, Simon Williams, Dieter Platzek, Antje Mrotzek, Yu Zhang, Carlo Gatti, Eckhard Muller, Mamoun Muhammed, Michael Rowe, Journal of Applied Physics 93 (1) (2003).
[120] Xie Jian, Zhao Xin Bing, Mi Jian Li, Cao Gao Shao, Tu Jian Ping, ISSN (2004) 1009–3095.
[121] Qinyu He, Qing Hao, Xiaowei Wangm, Jian Yang, Yucheng Lan, Xiao Yan, Bo Yu, Yi Ma, Bed Poudel, Giri Joshi, Dezhi Wang, Gang Chen, Zhifeng Ren, Journal of Nanoscience and Nanotechnology 8 (2008) 4003–4006.
[122] Alexander A. Balandin, Olga L. Lazarenkova, Applied Physics Letters 82 (3) (2003).
[123] Alexander Balandin, Kang L. Wang, Physical Review B 58 (3) (1998).
[124] Weili Manu Shamsa, Liu, Alexander A. Balandina, Jianlin Liu, Applied Physics Letter 87 (2005).
[125] A. Khitun, A. Balandin, K.L. Wang, G. Chen, Physica E 8 (2000) 13–18.
[126] A. Khitun, A. Balandin, J.L. Liu, K.L. Wang, Journal of Applied Physics 88 (2) (2000).
[127] Yu Ming Lin, M.S. Dresselhaus, Physical Review B 68 (2003).
[128] T.M. Tritt, M.G. Kanatzidis, H.B. Lyon, Mateials Research Society Proceedings 478 (1997).
[129] T.C. Harman, P.J. Taylor, M.P. Walsh, B.E. LaForge, Science 297 (2002).
[130] D.D.L. Wijngaards, S.H. Kong, M. Bartek, R.F. Wolffenbuttel, Sensors and Actuators 85 (2000) 316–322.
[131] G.Jeffrey Snyder, James R. Lim, Chen Kuo Huang, Jean Pierre Fleurial, Nature Materials 2 (2003).
[132] Daryoosh Vashaee, Ali shakouri, Physical Review Letters 92 (10) (2004).
[133] Herald Bottner, Joachim Nurnus, Alexander Gavrikov, Gerd Kuhner, Martin Jagle, Christa Kunzel, Dietmar Eberhard, Gerd Plescher, Axel Schubert, Karl-Heinz Schlereth, Journal of Microelectromechanical Systems 13 (2004)3 13 (2004).
[134] D.M. Rowe, CRC Handbook of Thermoelectrics, CRC Press, Danvers, MA, USA, 1995. ISBN: 0-8493-0146-7.
[135] Shengnan Zhanga, Jian Hea, Journal of the South Carolina Academy of Science 6 (2) (2008) 14.
[136] X.B. Zhao, X.H. Ji, Y.H. Zhng, T.J. Zhu, J.P. Tu, X.B. Zhang, Applied Physics Letter 86 (2005).
[137] Bed Paudel, Qing Hao, Yi Ma, Yucheng Lan, Austin Minnich, Bo Yu, Xian Yan, Dezhi Wang, Andrew Muto, Daryoosh Vashaee, Xiaoyan Chen, Junming Liu, M.S. Dresselhaus, Gang Chen, Zhifeng Ren, High Thermoelectric Performance of Nanostructured Bismuth Antimony Telluride Bulk alloys, Sciencexpress, March 2008.
[138] Qian Zhang, Qinyong Zhang, Shuo Chen, Weishu Liu, Kevin Lukas, Xiao Yan, Hengzhi Wang, Dezhi Wang, Cyril Opeil, Gang Chen, Zhieng Ren, Nano Energy 1 (2012) 183–189.
[139] Li Ping Tana, Ting Suna, Shufen Fana, Lay Yong Nga, Ady Suwardia, Qingyu Yana, Huey Hoon Hng, Nano Energy Available online 17 (2012).
[140] Feng-Jia Fan, Bo Yu, Yi-Xiu Wang, Yan-Long Zhu, Xiao-Jing Liu, Shu-Hong Yu, Zhifeng Ren, Journal of American Chemical Society 133 (2011) 15910–15913.
[141] H. Grimm, N. Petermann, A. Gupta, H. Wiggers, NSTI-Nanotech 1 (2010) 201.
[142] M. Scheele, N. Oeschler, I. Veremchuk, K.G. Reinsberg, A.M. Kreuziger, A. Kornowski, J. Broekaert, C. Klinke, H. Weller, ACS Nano 4 (7) (2010) 4283–4291 July 27.
[143] Ya Yang, Ken C. Pradel, Qingshen Jing, Jyh Ming Wu, Fang Zhang, Yusheng Zhou, Yue Zhang, Zhong Lin Wang, ASC Nano 6 (June 29, 2012) 6984–6989.
[144] M. Zhou, H. Zhu, Y. Jiao, Y. Rao, S. Hark, Y. Liu, L. Peng, Q. Li, Journal of Physical Chemistry C 113 (2009) 8945–8947.
[145] Qing Hao, Gaohua Zhu, Giri Joshi, Xiaowei Wang, Austin Minnich, Zhifeng Ren, Gang Chen, Applied Physics Letters 97 (2010).
[146] Zhao Ajay Soni, Yu Yanyuan, Michael Khor Ligen, Aik Khiam, S.Dresselhaus Mildred, Xiong Qihua, Enhanced Thermoelectric Properties of Solution Grown Bi2Te3−xSex Nanoplatelet Composites, Nano Letter, ACS Publications, 2012 12, 1203−1209.
[147] Jing Liu, et al., Key Engineering Materials 280–283 (2005) 397.
[148] H.Y. Chen, X.B. Zhao, Y.F. Lu, E. Mueller, A. Mrotzek, Journal of Applied Physics 94 (2003) 6621.
[149] Tie-Jun Zhu, Yi-Qi Cao, Qian Zhang, Xin-Bing Zhao, Journal of Electronic Materials 39 (9) (2010) 1990–1995.
[150] J.L. Harringa, B.A. Cook, in: D.M. Rowe (Ed.), Solid-State Synthesis of Thermoelectric Materials (Thermoelectrics Handbook—Macro to Nano), CRC Press, 2005.
[151] Giri Joshi, Hohyun Lee, Yucheng Lan, Xianwei Wang, Gaohua Zhu, Dezhi Wang, Ryan W Gould, Diana C Cuff, Ming Y Tang, Mildred S Dresselhaus, Gang Chen, Zhifeng Ren, Nano Letters 8 (12) (2008) 4670–4674.
[152] Yucheng Lan, Austin Jerome Minnich, Gang Chen, Zhifeng Ren, Advanced Functional Materials 20 (2010) 357–376.
[153] C.B. Murray, C.R. Kagan, M.G. Bawendi, Annual Review of Materials Science 30 (2000) 545.
[154] Alexis R. Abramson, Woo Chul Kim, Scott T. Huxtable, Haoquan Yan, Yiying Wu, Arun Majumdar, Chang-Lin Tien, Peidong Yang, Journal Of Microelectromechanical System S 13 (3) (2004).
[155] Peixin Zhu, Takahiro Takeuchi, Hiromichi Ohta, Won-Seon Seo, Kunihito Koumoto, Materials Transactions 46 (7) (2005) 1453–1455.
[156] Feng-Jia Fan, Yi-Xiu Wang, Xiao-Jing Liu, Liang Wu, Shu-Hong Yu, Advanced Materials (2012).
[157] M. Zebarjadi, K. Esfarjani, M.S. Dresselhaus, Z.F. Ren, G. Chen, Energy & Environmental Science 5 (2012) 5147–5162.
[158] Chris Gould, Noel Shammas, A Review of Thermoelectric MEMS Devices for Micro, Power Generation, Heating and Cooling Applications, Source: icro Electronic and Mechanical

Please cite this article as: H. Alam, S. Ramakrishna, A review on the enhancement of figure of merit from bulk to nano-thermoelectric materials, Nano Energy (2013), http://dx.doi.org/10.1016/j.nanoen.2012.10.005

Systems, Kenichi Takahata (Ed.), ISBN 978-953, 307-027, 2009.
[159] A.J. Minnich, M.S. Dresselhaus, Z.F. Ren, G. Chen, Energy & Environmental Science 2 (2009) 66-479.
[160] Allon I. Hochbaum, Renkun Chen, Raul Diaz Delgado, Wenjie Liang, Erik C. Garnett, Mark Najarian, Arun Majumdar, Peidong Yang, Nature 45 (2008) 163-168.

Mr. Hilaal Alam is currently working in Qtech Nanosystems, Singapore on nanopositioning technology. He earned his Bachelor of Engineering from Rashtreeya Vidyalaya College of Engineering, Bangalore University, India and M.S. from Indian Institute of Technology Madras, Chennai, India. He is currently working on nanocomposite thermoelectric materials for CMOS. His research interests cover the flexures, nanopositioning and MEMS.

Professor Seeram Ramakrishna FREng, FNAE, FIES, is the Director of Centre for Nanofibers & Nanotechnology at the National University of Singapore. He is considered as the father of electrospun nanomaterials for pioneering applications. He has authored 5 books and ~500 peer reviewed papers, which attracted ~20,000 citations with an Hindex of 70. Various global databases including Thomson Reuters ISI Web of Knowledge, Elsevier Scopus, and Microsoft Academic place him among the top 25 Materials Scientists worldwide. As a founding chairman he championed the establishment of ~$120 million Solar Energy Research Institute of Singapore, SERIS. He served on the panels of International Atomic Energy Agency, IAEA and Singapore Energy Advisory Committee. He is a board member of Asia Society for Innovation & Policy, and speaker on global trends at meetings facilitated by Think tanks, Governments, World Bank, EU, OECD, ASEAN, tertiary education providers, and Academies. He authored the book 'The Changing Face of Innovation'. He has 15 years of senior management experience at the National University of Singapore: University Vice-President (Research Strategy); Dean of Engineering; Director of NUS Enterprise, Director of Industry & Technology Relations Office; Founding Director of NUS Bioengineering; Founding Director of NUS initiative on Nanoscience & Nanotechnology, NUSSNI; and Board member of national organizations, policy institutes & tertiary education institutions. He received Ph.D. degree from the University of Cambridge, and the general management training from the Harvard University. He is an elected international fellow of Royal Academy of Engineering, UK; National Academy of Engineering, India; Institution of Engineers Singapore; ASEAN Academy of Engineering & Technology; American Association of the Advancement of Science; ASM International; American Society for Mechanical Engineers; American Institute for Medical & Biological Engineering; Institution of Mechanical Engineers, UK; and Institute of Materials, Minerals & Mining, UK.

Please cite this article as: H. Alam, S. Ramakrishna, A review on the enhancement of figure of merit from bulk to nano-thermoelectric materials, Nano Energy (2013), http://dx.doi.org/10.1016/j.nanoen.2012.10.005